Single synapse indicators of glutamate release and uptake in acute brain slices from normal and Huntington mice
--Manuscript Draft--

Article Type:	Invited Methods Article - JoVE Produced Video
Manuscript Number:	JoVE60113R2
Full Title:	Single synapse indicators of glutamate release and uptake in acute brain slices from normal and Huntington mice
Section/Category:	JoVE Neuroscience
Keywords:	Glutamate release, glutamate clearance, glutamate spread, presynaptic terminal, astrocyte, glutamate uptake, decay kinetics, spill-over, optogenetics, iGluu, sCMOS
Corresponding Author:	Rosemarie Grantyn GERMANY
Corresponding Author's Institution:	
Corresponding Author E-Mail:	rosemarie.grantyn@charite.de
Order of Authors:	Anton Dvorzhak
	Rosemarie Grantyn
Additional Information:	
Question	Response
Please indicate whether this article will be Standard Access or Open Access.	Standard Access (US$2,400)
Please indicate the **city, state/province, and country** where this article will be **filmed**. Please do not use abbreviations.	Berlin Germany

1   **TITLE:**
2   Single Synapse Indicators of Glutamate Release and Uptake in Acute Brain Slices from Normal
3   and Huntington Mice
4
5   **AUTHORS& AFFILIATIONS:**
6   Anton Dvorzhak[1], Rosemarie Grantyn[1]
7
8   [1]Synaptic Dysfunction Group, Neuroscience Research Center, Charité - University Medicine,
9   Berlin, Germany
10
11 **Email Addresses of Co-Authors:**
12 Anton Dvorzhak   (anton.dvorzhak@charite.de)
13
14 **Corresponding Author:**
15 Rosemarie Grantyn   (rosemarie.grantyn@charite.de)
16

17 **KEYWORDS:**
18 Glutamate release, glutamate clearance, glutamate spread, presynaptic terminal, astrocyte,
19 glutamate uptake, decay kinetics, spill-over, optogenetics, $iGlu_u$, sCMOS
20

21 **SUMMARY:**
22 We present a protocol to evaluate the balance between glutamate release and clearance at
23 single corticostriatal glutamatergic synapses in acute slices from adult mice. This protocol uses
24 the fluorescent sensor $iGlu_u$ for glutamate detection, a sCMOS camera for signal acquisition and
25 a device for focal laser illumination.
26

27 **ABSTRACT:**
28 Synapses are highly compartmentalized functional units that operate independently on each
29 other. In Huntington's disease (HD) and other neurodegenerative disorders, this independence
30 might be compromised due to insufficient glutamate clearance and the resulting spill-in and
31 spill-out effects. Altered astrocytic coverage of the presynaptic terminals and/or dendritic
32 spines as well as a reduced size of glutamate transporter clusters at glutamate release sites
33 have been implicated in the pathogenesis of diseases resulting in symptoms of dys-
34 /hyperkinesia. However, the mechanisms leading to the dysfunction of glutamatergic synapses
35 in HD are not well understood. Improving and applying synapse imaging we have obtained data
36 shedding new light on the mechanisms impeding the initiation of movements. Here, we
37 describe the principle elements of a relatively inexpensive approach to achieve single synapse
38 resolution by using the new genetically encoded ultrafast glutamate sensor $iGlu_u$, wide-field
39 optics, a scientific CMOS (sCMOS) camera, a 473 nm laser and a laser positioning system to
40 evaluate the state of corticostriatal synapses in acute slices from age appropriate healthy or
41 diseased mice. Glutamate transients were constructed from single or multiple pixels to obtain
42 estimates of i) glutamate release based on the maximal elevation of the glutamate
43 concentration [Glu] next to the active zone and ii) glutamate uptake as reflected in the time
44 constant of decay (TauD) of the perisynaptic [Glu]. Differences in the resting bouton size and

45   contrasting patterns of short-term plasticity served as criteria for the identification of
46   corticostriatal terminals as belonging to the intratelencephalic (IT) or the pyramidal tract (PT)
47   pathway. Using these methods, we discovered that in symptomatic HD mice ~40% of PT-type
48   corticostriatal synapses exhibited insufficient glutamate clearance, suggesting that these
49   synapses might be at risk to excitotoxic damage. The results underline the usefulness of TauD
50   as a biomarker of dysfunctional synapses in Huntington mice with a hypokinetic phenotype.
51
52   **INTRODUCTION:**
53   The relative impact of each synaptic terminal belonging to a "unitary connection" (i.e., the
54   connection between 2 nerve cells) is typically assessed by its influence on the initial segment of
55   the postsynaptic neuron[1,2]. Somatic and/or dendritic recordings from postsynaptic neurons
56   represent the most common and, until now, also the most productive means to clarify
57   information processing under a top-down or vertical perspective[3-5]. However, the presence of
58   astrocytes with their discrete and (in rodents) non-overlapping territories may contribute a
59   horizontal perspective that is based on local mechanisms of signal exchange, integration and
60   synchronization at synaptic sites[6-10].
61
62   Because it is known that astroglia play, in general, a major role in the pathogenesis of
63   neurodegenerative disease[11,12] and, in particular, a role in the maintenance and plasticity of
64   glutamatergic synapses[13-16], it is conceivable that alterations in synaptic performance evolve in
65   accordance with the state of astrocytes in the shared target area of afferent fibers with diverse
66   origin. To further explore the target-/astroglia-derived local regulatory mechanisms in health
67   and disease, it is necessary to evaluate individual synapses. The present approach was worked
68   out to estimate the range of functional glutamate release and clearance indicators and to
69   define criteria that may be used to identify dysfunctional (or recovered) synapses in brain areas
70   most closely related to movement initiation (i.e., first of all in the motor cortex and dorsal
71   striatum).
72
73   The striatum lacks intrinsic glutamatergic neurons. Therefore, it is relatively easy to identify
74   glutamatergic afferents of extrastriatal origin. The latter mostly originate in the medial
75   thalamus and in the cerebral cortex (see[17-20] for more). Corticostriatal synapses are formed by
76   the axons of pyramidal neurons localized in cortical layers 2/3 and 5. The respective axons form
77   bilateral intra-telencephalic (IT) connections or ipsilateral connections via a fiber system that
78   more caudally constitutes the pyramidal tract (PT). It has further been suggested that IT- and
79   PT-type terminals differ in their release characteristics and size[21,22]. In view of these data, one
80   could also expect some differences in the handling of glutamate.
81
82   The striatum is the most affected brain area in Huntington's disease (HD)[5]. Human HD is a
83   severe genetically inherited neurodegenerative disorder. The Q175 mouse model offers an
84   opportunity to investigate the cellular basis of the hypokinetic-rigid form of HD, a state that has
85   much in common with parkinsonism. Starting at an age of about 1 year, homozygote Q175 mice
86   (HOM) exhibit signs of hypokinesia, as revealed by measuring the time spent without
87   movement in an open field[23]. The present experiments with heterozygote Q175 mice (HET)
88   confirmed the previous motor deficits observed in HOM and, in addition, showed that the

89   observed motor deficits were accompanied by a reduced level of the astrocytic excitatory
90   amino acid transporter 2 protein (EAAT2) in the immediate vicinity of corticostriatal synaptic
91   terminals[24]. It has therefore been hypothesized that a deficit in astrocytic glutamate uptake
92   could lead to dysfunction or even loss of respective synapses[25,26].
93
94   Here, we describe a new approach that allows one to evaluate single synapse glutamate
95   clearance relative to the amount of the released neurotransmitter. The new glutamate sensor
96   iGlu$_u$ was expressed in corticostriatal pyramidal neurons. It was developed by Katalin Török[27]
97   and represents a modification of the previously introduced high-affinity but slow glutamate
98   sensor iGluSnFR[28]. Both sensors are derivatives of the enhanced green fluorescent protein
99   (EGFP). For spectral and kinetic characteristics, see Helassa et al.[27]. Briefly, iGlu$_u$ is a low-affinity
100 sensor with rapid de-activation kinetics and therefore particularly well suited to study
101 glutamate clearance at glutamate-releasing synaptic terminals. The dissociation time constant
102 of iGlu$_u$ was determined in a stopped-flow device, which rendered a Tau$_{off}$ value of 2.1 ms at 20
103 °C, but 0.68 ms when extrapolated to a temperature of 34 °C[27]. Single Schaffer collateral
104 terminals probed at 34 °C with spiral laser scanning in the CA1 region of organotypic
105 hippocampal cultures under a 2-photon microscope exhibited a mean time constant of decay of
106 2.7 ms.
107
108 **PROTOCOL:**
109
110 All work has been carried out in accordance with the EU Directive *2010/63/EU* for animal
111 experiments and was registered at the Berlin Office of Health Protection and Technical Safety
112 (G0233/14 and G0218/17).
113
114 NOTE: Recordings from Q175 wild-type (WT) and heterozygotes (HETs) can be performed at any
115 age and sex. Here we studied males and females at an age of 51 to 76 weeks.
116
117 **1. Injection of the glutamate sensor iGlu$_u$ for expression in corticostriatal axons**
118
119 1.1. Use the pipette puller (one step mode) to prepare borosilicate glass pipettes for the
120 injection of the virus. After pulling, break the pipette manually to obtain a tip diameter of 30–
121 50 µm. Autoclave the pipette and surgical instruments, including the drill for opening the skull.
122
123 1.2. Store the virus AAV9-CaMKIIa.iGlu$_u$.WPRE-hGH (7.5 x 10^{13}gc/mL) at -80 °C in 10 µL aliquots.
124 If injections are performed shortly after virus production (within 6 months), keep at 5 °C. Before
125 surgery, take out the vial and maintain it at room temperature.
126
127 1.3. Fill the glass pipette and remove any bubbles.
128
129 1.4. Anesthetize the animal with an intraperitoneal injection of a solution containing 87.5
130 mg/kg ketamine and 12.5 mg/kg xylazine. Subcutaneously inject 0.25% bupivacain (8 mg/kg) for
131 additional pain relief. Check the depth of anesthesia by monitoring the muscle tone and
132 observing the absence of pain-induced reflexes.

133

134 1.5. Shave the skin on the head and sterilize it with 70% alcohol. Fit the mouse into the
135 stereotaxic frame.

136

137 1.6. Use a scalpel to remove the skin and a high speed (38,000 rpm) –drill to make a 1.2 mm
138 hole in the bone above the motor cortex.

139

140 1.7. Mount the syringe with the attached injection pipette in the holder of a precision
141 manipulator. Insert the vertically oriented pipette into the cortex at 4 different sites. The
142 injection coordinates are, with respect to bregma (in mm): anterior 1.5, lateral 1.56, 1.8, 2.04,
143 2.28. The depth with respect to *dura mater* is (in mm): 1.5–1.7.

144

145 1.8. Using the injection system, inject 0.3 µL per site of the undiluted virus solution with a
146 velocity of 0.05 µL/min. After each injection, leave the pipette in place for 1 min before
147 withdrawing it slowly (1 mm/min).

148

149 1.9. Finish by closing the surgical wound with a nylon suture.

150

151 1.10. Leave the mouse for 0.5 to 1 h on a heating pad in a clean cage before returning it to its
152 original cage.

153

154 1.11. Maintain the mouse on a 12 h day-night cycle for 6 to 8 weeks before the preparation of
155 acute brain slices.

156

157 NOTE: To avoid immune reactions resulting in cell damage and synapse loss, injection of
158 multiple viral constructs must be performed simultaneously or within 2–3 hours after the
159 primary injection. The coordinates for iGlu$_u$ injection were selected according to the Paxinos
160 and Franklin[29] brain atlas. They correspond to the M1 motor cortex. Immunostaining of injected
161 brains visualized numerous but mostly well isolated axons and axon varicosities in the ipsi- and
162 contralateral striatum and in the contralateral M1 and S1 cortices.

163

164 **2. Search for glutamatergic terminals expressing the glutamate sensor iGlu$_u$**

165

166 **2.1. Calibration mode**

167

168 2.1.1. Prepare the sCMOS camera and the camera control software with the following settings.
169 On the **Readout** page set **Pixel readout rate**: 560 MHz (= fastest readout), **Sensitivity/Dynamic**
170 **Range**: bit, **Spurious Noise Filter**: Yes, **Overlap Readout**: Yes. On the **Binning/ROI** page, select
171 **Full screen.**

172

173 2.1.2. Prepare a glass slide containing a drop of 5 mg/mL Lucifer Yellow (LY) under a cover slip.

174

175 2.1.3. Place the LY slide under a 63x objective, open the laser shutter and perform a serial
176 acquisition using the following settings: **Pixel Binning**: 1x1, **Trigger mode**: Internal, **Exposure**

177 **time**: Minimal (to be determined).

178

179 2.1.4. Adjust the laser power to produce a fluorescence spot of 4 µm in diameter (the image
180 should not contain saturated pixels).

181

182 2.1.5. To perform a calibration of the laser positioning system, select the following settings in
183 the laser positioning software: **Spot-size diameter**: 10, **Scanning velocity**: 43.200 kHz. Click the
184 **Start image acquisition** button on the right panel. Set **Runs**: 0, **Run delay**: 0, and select the **Run**
185 **at TTL** option on the **Sequence** page. Click the **Calibrate button** on the Calibration page and
186 calibrate the laser control software according instructions shown in the top-left corner of the
187 acquisition screen.

188

189 2.1.6. If the setup uses independent software for camera and laser control, acquire screenshots
190 from the camera acquisition window and send it to the laser control software for a re-
191 calculation of the XY coordinates. If the software is installed on different computers, then use a
192 video grabber to import the image into the laser control software. The laser control software
193 will need the information on the XY scaling factors and offsets. For this purpose, determine the
194 coordinates of the top-left, bottom-left and bottom-right corners of the image within the
195 acquisition window of the laser control program. Calculate the scaling factors according to the
196 following equations: X factor = (X bottom-right – X bottom-left)/2048, X offset = X bottom-left,
197 Y factor = (Y top-left – Y bottom-left)/2048, Y offset = Y bottom-left.

198

199 2.1.7. At the end of the calibration procedure, create a rectangular region of interest (ROI) of
200 267x460 pixels, move it to the center of the screen and click the **Start sequence** button.

201

202 2.1.8. Return to the following camera control software settings: **Binning**: 2x2, **Trigger mode**:
203 External exposure, **Exposure time**: Minimal (to be determined).

204

205 **2.2 Autofluorescence correction mode**

206

207 NOTE: The resting level of [Glu] in the environment of active synaptic terminals is typically
208 below 100 nM[14,30-34]. Accordingly, any sensor of glutamate, especially a low affinity sensor like
209 $iGlu_u$ will be rather dim in the absence of synaptic glutamate release. Nevertheless, some $iGlu_u$
210 fluorescence can even be detected at rest, but must be distinguished from the tissue
211 autofluorescence. The 473 nm illumination elicits both $iGlu_u$ fluorescence and autofluorescence
212 (**Figure 1A–C**). The latter occupies a wide range of wavelengths, while $iGlu_u$ fluorescence is
213 limited to 480–580 nm (with a maximum at 510 nm). The correction for autofluorescence is
214 based on the acquisition of two images with different high-pass filters.

215

216 2.2.1. Prepare brain slices in advance as described elsewhere[35]. Keep bran slices ready.

217

218 2.2.2. Transfer the slices into the recording chamber, submerging them into oxygenized
219 artificial cerebrospinalfluid (ACSF) containing 125 mM NaCl, 3 mM KCl, 1.25 mM NaH_2PO_4, 25
220 mM $NaHCO_3$, 2 mM $CaCl_2$, 1 mM $MgCl_2$, 10 mM glucose (pH 7.3, 303 mOsm/L), supplemented

221 with 0.5 mM sodium pyruvate, 2.8 mM sodium ascorbate and 0.005 mM glutathione. Use a
222 flow rate of 1–2 mL/min. Keep the bath temperature at 28–30 °C.

224 2.2.3. Locate the dorsal striatum under a 20x water immersion objective. Fix the slices with a
225 nylon grid on a platinum harp to minimize the tissue movement. Switch to the 63x /NA 1.0
226 water immersion objective. Select filters reflecting light at 473 nm (dichroic mirror) and passing
227 light with wavelengths >510 nm (emission filter).

229 2.2.4. Synchronize illumination, stimulation and image acquisition using an AD/DA board with
230 the respective control software. Set the trigger program to control acquisition with a laser
231 exposure time of 180 ms and an image acquisition time of 160 ms. Use the laser positioning
232 device to send the laser beam to a predetermined number of points and define the settings for
233 **Scanning velocity** and **Spot size**.

235 2.2.5. Acquire an image of both autofluorescence and $iGlu_u$ -positive structures using a high
236 pass filter at 510 nm ("yellow image").

238 2.2.6. Acquire an image with autofluorescence alone using a high-pass filter at 600 nm ("red
239 image").

241 2.2.7. Scale the red and yellow images, using the mean intensities of the 10 brightest and the 10
242 darkest pixels to define the range. Perform a subtraction "yellow minus red image" and rescale
243 the subtracted image to generate a standard 8-bit tif file for convenient visualization of the
244 bouton of interest (**Figure 1D**). It contains the bright pixels from the $iGlu_u$-positive structures,
245 grey pixels from the background and dark pixels from structures with autofluorescence.

247 NOTE: With the given equipment the mean resting fluorescence (F) will be below 700 A.U.

249 **2.3 Bouton search mode**

251 NOTE: $iGlu_u$-positive pixels may belong to functionally different elements of the axonal tree,
252 such as axon branches of different order, sites of bifurcation, varicosities after vesicle depletion
253 or fully active varicosities. However, it is almost impossible to identify functional synaptic
254 terminals just by visual inspection. Therefore, each glutamatergic synaptic terminal needs
255 identification by its responsiveness to electrical depolarization. Sites that do not respond to
256 stimulation have to be discarded. The physiological means to induce glutamate release from
257 corticostriatal axons is to elicit an action potential. This can either be achieved by using a
258 channel rhodopsin of appropriate spectral characteristics or by electrical stimulation of an axon
259 visualized by $iGlu_u$ itself. To avoid accidental opsin activation, we preferred the latter
260 approastep

262 2.3.1. Use the micropipette puller (in a four-step mode) to produce stimulation pipettes from
263 borosilicate glass capillaries. The internal tip diameter should be about 1 μm. When filled with
264 ACSF, the electrode resistance should be about 10 MΩ.

265

2.3.2. To induce the action potential-dependent release of glutamate from a set of synaptic boutons attached to the same axon, use 63x magnification, the 510 nm emission filter and the subtracted image to place a glass stimulation electrode next to a fluorescent varicosity. Avoid the proximity of additional axons.

2.3.3 Turn on the stimulator to deliver depolarizing current pulses to the stimulation pipette. Use current intensities around 2 µA (no more than 10 µA).

2.3.4. Turn on the multi-channel bath application system where one channel delivers the standard bath solution and the other channels deliver the necessary blockers of ion channels, transporters or membrane receptors. Control the flow at the site of recording and then switch to the tetrodotoxin (TTX) channel (bath solution plus 1 µM TTX). After 2-3 min, stimulate the bouton of interest again, but now in the absence of action potential generation. The release is directly due to calcium influx through voltage-depended calcium channels.

2.3.5. By turning the intensity key on the stimulator, adjust the stimulation current to obtain responses similar to those elicited via action potentials. Typically, the stimulation current would be around 6 µA for a 0.5 ms depolarization.

2.3.6. For basic testing of the preparation, apply 0.5 mM $CdCl_2$. The presence of this calcium channel blocker glutamate release completely prevents the synaptic glutamate release thereby validating the calcium dependence of the directly evoked glutamate signal.

NOTE: The following general recommendation may help to increase the success rate of single synapse experiments in the striatum. To select glutamatergic synaptic terminals with intact release machinery, a varicosity should: (i) Have a smooth spindle-like shape; (ii) Not be associated with an axon bifurcation; (iii) Be brighter than other structures on the "yellow image"; (iv) Reside in the striatal neuropil rather than in the fiber tracts; (v) Reside on a very thin axon branch; (vi) Not reside within the deeper parts of the slice.

3. Visualization of glutamate release and clearance

3.1. Recording mode

NOTE: After the subtraction of the autofluorescence (step 2.2) and a few initial tests for responsiveness of the bouton of interest (Step 2.3), data acquisition can begin. The responses to electrical activation of glutamate release from single axon terminals can be observed in the image directly (**Figure 2**), without applying further analysis tools. However, it proved to be very convenient to immediately extract some basic indicators of synapse performance (**Figure 3**). This information is needed to make decisions on subsequent course of experiment, such as selection of particular terminal types, rapid assessment of HD-related alterations, the number and frequency of trials or drugs to be applied with the superfusion system. It might also be necessary to deal with eventually appearing artifacts. First, the standard settings for data

309   recording is described.

311   3.1.1. Using the microscope XY drives, place the tested iGlu$_u$-positive bouton close to the
312   viewfield center. Stop the image acquisition with the **Abort acquisition button**. On the last
313   acquired picture, determine the XY position of the resting bouton center by clicking on it with
314   the left mouse button. The XY coordinates of the set cursor will be shown on the bottom status
315   panel of the acquisition window.

317   3.1.2. Using the calibration data (step 2.1.6), calculate the coordinates of the site where the
318   laser beam should be sent for the excitation of the iGlu$_u$ fluorescence. Use the following
319   equations: X laser = X camera * X factor + X offset, Y laser= Y offset – Y camera * Y factor. While
320   performing this recalculation, pay attention to the vertical or horizontal flip settings of the
321   camera.

323   3.1.3. Create a one-point sequence in the laser control software using the calculated
324   coordinates. For this purpose, select **Point** in the **Add to sequence** box on the **Sequence page**
325   of the laser control software. Select 10 μs for the delay to trigger onset and 180 ms for the laser
326   pulse time. Move the mouse to the calculated coordinates and click left button.

328   3.1.4. Select the following settings in the laser control software: **Runs**: 0, **Run delay**: 0,
329   **Sequence**: Run at TTL. Then click **Start sequence**.

331   3.1.5. In the camera control software, select the following settings. On the **Binning/ROI** page,
332   set **Image Area**: Custom, **Pixel Binning**: 2x2, **Height**: 20, **Width:** 20, **Left**: X-coordinate of the
333   resting iGlu$_u$-positive spot minus 10 px, **Bottom:** Y-coordinate of the resting iGlu$_u$-positive spot
334   minus 10 px, **Acquisition Mode:** Kinetic Series, **Kinetic Series Length**: 400, **Exposure Time**:
335   0.0003744s (minimal value). With such settings, the acquisition rate will be 2.48 kHz.

337   3.1.6. Select **Trigger mode**: External. Click **Take signal** in the camera control software. Initiate
338   the experimental protocol laid down for the trigger device.

340   3.1.7. Implement the experimental protocol **Trial** with the following time line: 0 ms – start trial,
341   1 ms – start laser illumination, 20 ms – start image acquisition with camera, 70 ms – start
342   electrical stimulation 1, 120 – start electrical stimulation 2, 181 ms – end trial (laser and camera
343   off). Thus, during one trial the camera acquires 400 frames with a frequency of 2.48 kHz. See
344   steps 2.3.3 and 2.3.5. for details on electrical stimulation.

346   3.1.8. To allow for sufficient recovery of presynaptic vesicle pools, apply the protocol **Trial** with
347   a repetition frequency of 0.1 Hz or lower.

349   **3.2 Off-line construction of the glutamate transient and rapid assessment of glutamate**
350   **release and clearance for the identification of pathological synapses**

352   3.2.1. Turn on the evaluation routines. Here, we use an in-house-written software SynBout v.

353 3.2. (author: Anton Dvorzhak). The following steps are needed to construct a ΔF/F transient
354 from the pixels with elevated iGlu$_u$ fluorescence as in the video of **Figure 2.**

356 3.2.2 To determinate the bouton size, calculate the mean and standard deviation (SD) of the
357 ROI fluorescence intensity at rest (F), before the onset of stimulation. Determine and box the
358 area occupied by pixels with F>mean + 3 SD (**Figure 3A**). Determine a virtual diameter (in μm)
359 assuming a circular form of the supra-threshold area.

361 3.2.3. Determine ΔF as the difference between the peak intensity value and F. Plot the
362 stimulating current and ΔF/F against time (**Figure 3B**). Calculate the SD of ΔF/F at rest (before
363 the onset of stimulation) and the *Peak amplitude.* Use pixel with peak amplitude more than 3
364 SD of ΔF/F to perform monoexponential fitting for the decay from peak. Determine the time
365 constant of decay *TauD* of ΔF/F.

367 3.2.4. To estimate the *Maximal amplitude* at a given synapse, select the pixel with the highest
368 ΔF/F value. It is typically located within or next to the boundaries of the resting bouton iGlu$_u$
369 fluorescence. The *Maximal amplitude* would be the best indicator of the glutamate load
370 presented to the clearance machinery of a single synapse.

372 3.2.5. To estimate the spatial extension of the iGlu$_u$ signal, determine the diameter of the area
373 of all supra-threshold pixels combined to form a virtual circle. The respective diameter is called
374 *Spread*. The term *Peak s*pread then refers to the peak value of the averaged spread transient
375 (**Figure 3C**, difference between dotted red lines).

3.3 Corrections for possible artifacts

379 NOTE: Electrical depolarization is associated with an outward flow of the intra-pipette solution.
380 This may result in a small tissue displacement. To discriminate between stimulation-induced
381 changes of iGlu$_u$ and out-of-focus shifts of the image, one could use the following approach to
382 identify and to eliminate displacement artifacts (**Figure 4**).

384 3.3.1. Analyze the spatial characteristics of the suprathreshold pixels derived from a ROI with
385 signs of displacement (**Figure 4F–H**).

387 3.3.2. Find pixels outside the initially determined boundaries of the bouton at rest (**Figure 4F–H**,
388 boxed in red).

390 3.3.3. Identify eventually existing negative pixel intensity values (**Figure 4I, J**). Any ΔF/F in the
391 negative direction with an amplitude larger than the pre-stimulation mean ± 3 SD should be
392 regarded as artifact, and the record should be discarded.

394 3.3.4. To avoid out-of-focus artifacts, place the stimulation electrode on the antero-lateral side
395 of the synaptic bouton, use biphasic electrical stimulation and minimize the stimulation
396 intensity/duration.

397

398   NOTE: Out-of-focus artifacts can also be derived from the camera. If the latter is not optimally
399   fixed to the microscope it can produce oscillations, most likely due to small vibrations of the
400   camera cooling system. Such vibrations create a "yin and yang" pattern in the ΔF/F images
401   rotating with a frequency of 50 Hz. The vibrations can be mathematically subtracted from the
402   fluorescence signal, but the final quality of the measurements would then critically depend on
403   the recording time.

404

405   3.3.5. Fix the camera to the microscope such that vibrations are absent. If the latter remain,
406   place a rubber gasket between the camera and microscope adapter.

407

408   NOTE: One cannot neglect the possibility that the striatal neuropil around the synapse of
409   interest contains glutamatergic varicosities that do not express iGlu$_u$ and therefore remain
410   invisible. In the case of their co-activation (more likely in the absence of TTX) the transients
411   obtained from the boutons of interest might be affected by spill-over. The same applies to
412   iGlu$_u$-expressing terminals that were out of focus. A characteristic phenomenon would in this
413   case be that fluorescence transients originate from a much wider area. As this response is
414   eliminated by TTX, one can interpret it as an unspecific response induced by unwarranted
415   multi-fiber activation.

416

417   3.3.6. To correct for this unspecific multi-fiber response, follow the procedure outlined in **Figure
418   5**. Use the fluorescence signal of pixels at the viewfield boundaries. To minimize background
419   response, minimize stimulation intensity and duration or use TTX.

420

421   **REPRESENTATIVE RESULTS:**
422   **Identification of two types of corticostriatal glutamatergic varicosities**
423   IT and PT afferents originate in layer 2/3 and 5, respectively, and exhibit differential
424   ramification and termination patterns in the ipsilateral and contralateral (IT terminals only)
425   striatum. Still little is known about the properties of glutamate release and clearance under
426   repetitive activation conditions as observed during the initiation of movements, but it is well
427   documented that the respective glutamate-releasing varicosities differ in size[22]. Applying a size
428   criterion, it was found that IT and PT terminals exhibit contrasting forms of short-term
429   plasticity[24]. At stimulus intervals of 50 ms, the smaller IT terminals were prone to paired pulse
430   depression (PPD) while the larger PT terminals showed paired pulse facilitation. This difference
431   was also observed at shorter intervals (20 ms) and throughout a series of 6 pulses. **Figure 3** and
432   **Figure 6** illustrate these experiments where synaptic glutamate release was elicited via the
433   action potential mechanism at physiological Ca^{2+}/Mg^{2+} concentration.

434

435   **Identification of dysfunctional synapses in mice with advanced Huntington's disease**
436   Neurodegenerative diseases such as Alzheimer's, Parkinson's and Huntington's disease are
437   characterized by an ever progressing loss of glutamatergic synapses[36]. Novel therapies aim to
438   impede or even reverse this fatal progression. What exactly triggers the disappearance of a
439   synapse, and when, is largely unknown. Further insight can be expected from studies that offer
440   criteria for (a) the vital identification of a particular class of glutamatergic synapses and (b) the

441 detection of dysfunctional versus normally performing contacts. Here it will be shown how the
442 *TauD* values obtained from PT-type of terminals were used to estimate the fraction of
443 dysfunctional synapses in Q175 heterozygotes with an identified motor phenotype.
444
445 Prior to the single synapse imaging experiments, the mice were submitted to a rapid but rather
446 robust test for alterations in their exploratory behaviors. This test is called "step-over test". The
447 animal was placed into the center of a Petri dish (of 185 mm diameter and 28 mm wall height).
448 The test was recorded with a video camera. Using offline analysis, one can determine the time
449 between the take-off of the experimenter's hand and the moment when the animal has all 4
450 feet out of the dish. Plotting the data from over 100 WT and Q175 HET at ages between 12 and
451 18 months suggests that mice with a step-over latency of >300 s can be diagnosed as
452 hypokinetic. **Figure 7A** illustrates a significant positive correlation between the results obtained
453 for the total path run in the open field and the step-over latency.
454
455 Single synapse iGlu$_u$ imaging showed that these symptomatic HD mice exhibited a deficit in the
456 speed of juxtasynaptic glutamate decay as reflected in the *TauD* values from single (or first in a
457 sequence) stimuli (**Figure 7B,C**). In WT, such prolongation was only observed after the
458 application of a selective non-transportable inhibitor of glutamate uptake - DL-*threo*-β-
459 benzyloxyaspartic acid (TBOA, **Figure 7D,E**). This suggests a role of astrocytic glutamate
460 transporters in the regulation of synaptic glutamate clearance. Changes in the diffusion of Glu
461 in the perisynaptic space have not been found[24]. But, of course, much more work is needed to
462 actually identify the cause of slowed glutamate clearance in HD as well as in other forms of
463 parkinsonism. Apart from changes in the astrocyte proximity[9] and reduced *slc1A2* expression[37],
464 one may as well consider disease-related instability of EAAT2 in the plasma membrane of the
465 perisynaptic astrocyte processes (PAPs). This might be a result of changes in the EAAT2
466 interactome. Indeed, recent mass spectroscopy experiments in the lab point to a loss of EAAT2-
467 dystrophin interaction in striatal astrocytes (Hirschberg, Dvorzhak, Kirchner, Mertins and
468 Grantyn, unpublished).
469
470 Very little is known regarding the timeline of synaptic dysfunction with progression of HD, but it
471 is very likely that healthy synapses co-exist with already impaired ones. In searching for a
472 classification criterion, we examined the *TauD* data from different mice. For this purpose, the
473 amplitude and *TauD* values from 3 consecutive paired trials were normalized to the first
474 response (see **Figure 6F** for an experimental scheme), and the probability of occurrence of a
475 given *TauD* value was compared in age-matched WT versus Q175 HET (**Figure 6G**). It was found
476 that in WT *TauD* never exceeded 15 ms, while in symptomatic Q175 HET, 40% of the synapses
477 exhibited *TauD* values between 16 and 58 ms, despite a tendency for a reduction in the amount
478 of released glutamate (**Figure 6H,I**). *TauD* might then be regarded as a biomarker for
479 dysfunctional synapses in HD and further be used to verify functional recovery in experiments
480 targeting astrocytic glutamate transport.
481
482 **FIGURE LEGENDS:**
483
484 **Figure 1: Identification of iGlu$_u$-positive varicosities. (A**) Fluorescence image obtained with a

485 510 nm high pass filter ("yellow image"). (**B**) Same view field acquired with a 600 nm high pass
486 filter ("red image"). Note that that the spot marked with black arrowhead has disappeared in
487 (B). Overlay of (A) and (B). White arrow = autofluorescence, black arrow =iGlu$_u$-positive
488 varicosity. (**D**) Image obtained by subtraction of (B) from (A). The autofluorescent spots are dark
489 and the iGlu$_u$+ spot is bright.

491 **Figure 2: Movie still from a slow-motion video (slowdown factor 1240x).** Upper row: Images
492 from WT (left), Q175 HET (middle) and HOM (right). Lower row: Respective iGlu$_u$ transients
493 from the pixel with the highest glutamate elevation (*Maximal ΔF/F*). The red cursor indicates
494 the point on the transient corresponding to the image above the trace. note prolonged
495 elevation of iGlu$_u$ fluorescence (red pixels and ΔF/F transients). Modified and reprinted with
496 permission from Dvorzhak et al. [24]

498 **Figure 3: Extraction of functional indicators from single synapse images of the genetically**
499 **encoded ultrafast Glu sensor iGlu$_u$ in corticostriatal neurons**. (**A**, **D**) Example of a PT (A) and IT
500 (D) bouton with the respective iGlu$_u$ fluorescence at rest (left) and at the peak of an AP-
501 mediated iGlu$_u$ response (right). (**B**, **C**, **E**, **F**) iGlu$_u$ responses recorded from the bouton shown in
502 (A, D); Experiment in 2 mM Ca^{2+} and 1 mM Mg^{2+}. (**B**) Simultaneous recording of the stimulation
503 current (upper trace) and mean intensity of supra-threshold pixels (bottom trace). Same time
504 scale for all traces. Peak amplitudes (between dotted red horizontal lines) and a
505 monoexponential function fitted to the decay from this peak (red overlay). The corresponding
506 TauD (τ) values are shown next to the fitting curves. (**E**, **F**) Plot of spread against time. Peak
507 spread: difference between dotted red horizontal lines.

509 **Figure 4: Characteristics of a glutamate-induced iGlu$_u$ transient (A–E) as opposed to a**
510 **displacement artifact (F–J)**. (**A**, **B**) and (**F**, **G**) show the absolute fluorescence intensity at rest (A,
511 F) and after stimulation (B, G) in arbitrary units (au). (**C**, **H**) Fluorescence change in percent of
512 the resting fluorescence prior to stimulation (ΔF/F%). (**D**, **I**) Superposition of the iGlu$_u$ transients
513 from all pixels in arbitrary units. (**E**, **J**) Superposition of the iGlu$_u$ transients from all pixels in
514 ΔF/F %. In the case of synaptic glutamate release, the pixels next to the resting terminal exhibit
515 a fluorescence increase after stimulation, whereas in the case of out-of-focus shifts the
516 brightest pixel at rest merely change their position in the ROI, without an accompanying
517 increase in the over-all fluorescence intensity of the view-field. A displacement artifact can also
518 be recognized by the appearance of negative ΔF/F signals (J).

520 **Figure 5: Correction for unspecific iGlu$_u$ response**. (**A–D**) Example of paired synaptic response
521 contaminated by an unspecific background response. (**E–H**) Same after correction. (**A**, **E**) Before
522 stimulation. (**B**, **F**) During stimulation. (**C**, **G**) After stimulation. (**D**, **H**) Corresponding
523 superimposed intensity transients (in ΔF/F) from all pixels of the ROI. The timepoint of
524 acquisition of the images is marked by corresponding small letters over the arrowheads. Note
525 that in panel C the background response is very widespread and slowly decaying.

527 **Figure 6: Distinct size and size-related differences in the amplitude paired pulse ratio (PPR) of**
528 **the iGlu$_u$ transient**. (**A**) Simplified scheme of the corticostriatal circuitry[22], illustrating the

529 concept of preferential projection of pyramidal tract (PT) neurons to indirect pathway striatal
530 projection neurons (iSPNs) and intratelencephalic (IT) neurons to direct pathway SPNs (dSPNs),
531 with size-differences between the IT and PT terminals. (**B**) Bimodal distribution of bouton
532 diameters as determined by the supra-threshold resting fluorescence before stimulation.
533 Boutons with diameter ≥ 0.63 μm were defined as "Large" and assumed to be issued by PT
534 axons. For original images and specimen traces from PT- and IT-type of synapses see **Figure 3.**
535 (**C**) Significant positive correlation is seen between the PPR of peak amplitudes and the bouton
536 diameters. Each data point represents the average from the first 3 trials of each bouton.
537 *P<0.05, **P<0.01, ***P<0.001.

538

539 **Figure 7: Identification of dysfunctional synapses in Q175 mice with a hypokinetic phenotype**.
540 (**A**) Results of motor testing on the day of single synapse imaging. Step-over latencies >300 ms
541 were considered as pathological. At the age tested (average 16 months), 17/54 HET exhibited a
542 pronounced phenotype in the step-over test. With regard to hypokinesia, the step-over test
543 seems to be more sensitive than the open field test. Nevertheless, there was a significant
544 correlation between the outcome of the step-over test (time between placement and barrier
545 crossed with all four feet) and the open field test (i.e., total path run in 5 min). Y = -0.01511X +
546 458,7; P=0.0044 (simple regression). (**B**) Average evoked single synapse iGlu$_u$ transients
547 normalized to same peak amplitude to illustrate HD-related differences in the clearance of
548 synaptically released glutamate. The respective fitting curves highlight the differences in the
549 duration of the glutamate transients. (**C**) Quantification of the results from wild-type (grey), HET
550 (red) and HOM (magenta). (**D**, **E**) Incubation of WT slices in 100 nM of TFB-TBOA simulated the
551 depression of glutamate clearance observed in HOM. (**F**) Scheme of synapse activation and data
552 organization. (**G**) Cumulative histograms of #1 *TauD* values. (**H**, **I**) Plots of normalized #2
553 responses. Data from 31 WT and 30 HET synapses (all of PT type). In the WT sample all
554 TauDmax values were ≤15 ms. In the HET sample, 40% of synapses exhibited TauDmax values
555 exceeding the 15 ms threshold defined by the longest TauDmax in WT. These graphs emphasize
556 the HD-related differences in the ranges of maximal amplitude (i.e., the value from the pixel
557 with the highest iGlu$_u$ fluorescence increase) and TauDmax (the *TauD* of the pixel with the
558 highest elevation). TauDmax values exclusively encountered in HET are shown in red, and
559 amplitude values exclusively seen in WT are shown in grey. *P<0.05, **P<0.01, ***P<0.001. The
560 used statistical tests are indicated next to the respective graph.

561

562 **DISCUSSION:**
563 The experiments concern a question of general interest – synapse independency and its
564 possible loss in the course of neurodegeneration, and we describe a new approach to identify
565 affected synapses in acute brain slices from aged (>1 year) mice. Taking advantage of the
566 improved kinetic characteristics of the recently introduced glutamate sensor iGlu$_u$ the
567 experiments illuminate the relationship between synaptic glutamate release and uptake in a
568 way that has not been possible before.

569

570 The influence of glutamate clearance on the function and maintenance of synapses is not very
571 well elucidated, although the hypothesis that glutamate-induced excitotoxicity can cause
572 neuron loss and synapse pruning is mentioned in almost any pertinent review on epilepsy,

573 stroke and neurodegenerative diseases[38-41]. However, the available evidence is more limited
574 than possibly anticipated from the literature. Confusion is further added by the fact that the
575 selected experimental tools might be insufficient in view of the problems associated with low
576 spatial and temporal resolution when interpreting the results obtained with gross stimulation
577 and recording techniques[42,43]. This can lead to false negatives discouraging further research,
578 which is more than unfortunate in view of neurologic disorders as severe as Huntington's
579 disease. The present approach ensures better signal discrimination and therefore stronger
580 support of the idea that in HD a significant fraction of corticostriatal synapses exhibits signs of
581 impaired glutamate clearance.
582
583 The present results disclosed differences of short-term plasticity within the corticostriatal
584 pathway. Although the latter had been in the focus of numerous studies[17,44], it has not been
585 anticipated that the afferents originating from the upper cortical layers would exhibit
586 frequency-dependent depression, in contrast to pyramidal tract afferents originating in layer 5.
587 The latter preferentially showed a frequency-dependent potentiation of release and may
588 therefore be at higher risk for glutamate uptake insufficiency.
589
590 Experiments on acute brain slices from adult mice are important for elucidating synaptic
591 alterations at an appropriate age of life. The age and functional state of the preparation is
592 particularly relevant if astrocytes were involved in the mechanism of interest. Here, it is
593 essential that the astrocytes are mature enough to exhibit adult levels of glutamate transporter
594 activity and related chloride homeostasis[45].
595
596 Single synapse assays will pave the road towards a better understanding of HD-related changes
597 of glutamatergic synaptic transmission in the intact brain[46]. It has been shown that single
598 synapse resolution can also be achieved in the intact brain, provided that the synapses of
599 interest are localized in the superficial layers of the cerebral cortex[47].
600
601 Finally, the present experimental approach has the appeal that it can be used by many
602 followers, since the required equipment is still on the low-cost side.
603
604 In short, fluorescence signals reporting glutamate release and the juxtasynaptic changes in the
605 concentration of glutamate in the intact brain can provide data unachievable with any
606 electrophysiological method. But as with any new method, this approach has its limitations and
607 disadvantages that have in part been addressed in steps 2.2 and 3.3. The low resting
608 fluorescence of the fast and high affinity iGlu$_u$ sensor requires a bit of exercise/experience to
609 identify suitable varicosities for further testing. With co-expression of a genetically encoded
610 calcium indicator (GECI) such as XCaMP-R[48] and at least two coordinated lasers illumination
611 systems, the search of functional axon terminals would become much easier. In any case, it is
612 critical to expose the preparation as little as possible to the exciting light before and during
613 iGlu$_u$ recording.
614
615 The use of a 473 nm laser (instead of the regular whole field elimination) to elicit iGlu$_u$
616 fluorescence is a prerequisite for obtaining sufficient emission but will also cause bleaching.

617 Under the given conditions, $iGlu_u$ was fully bleached after 10 stimulation/acquisition trials (10
618 stimulus pairs at an inter-stimulus interval of 50 ms and a repetition rate of 1/10 s). The
619 maximal total illumination time for steady-state data acquisition with the presently used 1
620 photon laser system and the described setting was approximately 2 s. The bleaching of $iGlu_u$ is
621 exponential, being very strong during the first 20 ms after illumination start and much slower
622 thereafter. It is therefore advisable to avoid signal acquisition during the first 20 ms of each trial
623 and to acquire not more than a total of 10 response pairs. Responses to single stimuli could be
624 recorded with exposure times of 60-80 ms instead of the presently used 180 ms.
625
626 Another critical issue is the expression level of $iGlu_u$. In the pioneering study of Helassa et al.[27],
627 the viral constructs were applied by electroporation to cultured neurons[27], which produces
628 higher expression levels of the sensor and presumably also less bleaching especially if a two-
629 photon laser scanning device can be used instead of a one-photon microscope. Dürst et al.[49]
630 report routine acquisition of postsynaptic expression of $iGlu_u$ in CA1 pyramidal neurons in ~100
631 trials (each exposed for only 80 ms). However, cultured brain tissue is not an option when the
632 experiments aim at clarifying astrocyte-dependent synaptic functions in the aged brain. A
633 CaMKII-Cre-dependent expression of $iGlu_u$ using a stronger promoter may provide preparations
634 with stronger expression in fewer cells, thereby increasing the resolution of the method and
635 allowing for the acquisition of more trials per synapse.
636

645

646 **REFERENCE:**
647 1.   Magee, J.C. Dendritic integration of excitatory synaptic input. *Nature Reviews*
648 *Neuroscience.* **1**, 181-190 (2000).
649 2.   Thome, C. et al. Axon-carrying dendrites convey privileged synaptic input in
650 hippocampal neurons. *Neuron.* **83**, 1418-1430 (2014).
651 3.   Larkum, M.E., Petro, L.S., Sachdev, R.N.S., Muckli, L. A Perspective on Cortical Layering
652 and Layer-Spanning Neuronal Elements. *Frontiers in Neuroanatomy.* **12**, 56 (2018).
653 4.   Spruston, N. Pyramidal neurons: dendritic structure and synaptic integration. *Nature*
654 *Reviews Neuroscience.* **9**, 206-221 (2008).
655 5.   Khakh, B.S. et al. Unravelling and exploiting astrocyte dysfunction in Huntington's
656 disease. *Trends in Neurosciences.* **40**, 422-437 (2017).
657 6.   Perea, G., Navarrete, M., Araque, A. Tripartite synapses: astrocytes process and control
658 synaptic information. *Trends in Neurosciences.* **32**, 421-431 (2009).
659 7.   Perea, G., Araque, A. Astrocytes potentiate transmitter release at single hippocampal
660 synapses. *Science.* **317**, 1083-1086 (2007).

661   8.   Savtchenko, L.P. et al. Disentangling astroglial physiology with a realistic cell model in
662   silico. *Nature Communications.* **9**, 3554-05896 (2018).
663   9.   Octeau, J.C. et al. An optical neuron-astrocyte proximity assay at synaptic distance
664   scales. *Neuron.* **98**, 49-66 (2018).
665   10.   Verkhratsky, A., Nedergaard, M. Physiology of astroglia. *Physiological Reviews.* **98**, 239-
666   389 (2018).
667   11.   Xie, Z., Yang, Q., Song, D., Quan, Z., Qing, H. Optogenetic manipulation of astrocytes
668   from synapses to neuronal networks: A potential therapeutic strategy for neurodegenerative
669   diseases. *Glia.* **10** (2019).
670   12.   Verkhratsky, A., Parpura, V., Pekna, M., Pekny, M., Sofroniew, M. Glia in the
671   pathogenesis of neurodegenerative diseases. *Biochemical Society Transactions.* **42**, 1291-1301
672   (2014).
673   13.   Dvorzhak, A., Melnick, I., Grantyn, R. Astrocytes and presynaptic plasticity in the
674   striatum: Evidence and unanswered questions. *Brain Research Bulletin.* 17-25 (2017).
675   14.   Rose, C.R. et al. Astroglial Glutamate Signaling and Uptake in the Hippocampus.
676   *Frontiers in Molecular Neuroscience.* **10**, 451 (2018).
677   15.   Scimemi, A., Diamond, J.S. Deriving the time course of glutamate clearance with a
678   deconvolution analysis of astrocytic transporter currents. *Journal of Visualized Experiments.* **10**
679   (2013).
680   16.   Theodosis, D.T., Poulain, D.A., Oliet, S.H. Activity-dependent structural and functional
681   plasticity of astrocyte-neuron interactions. *Physiological Reviews.* **88**, 983-1008 (2008).
682   17.   Reiner, A., Deng, Y.P. Disrupted striatal neuron inputs and outputs in Huntington's
683   disease. *CNS Neuroscience & Therapeutics.* **24**, 250-280 (2018).
684   18.   Plotkin, J.L., Surmeier, D.J. Corticostriatal synaptic adaptations in Huntington's disease.
685   *Current Opinion in Neurobiology.* **33C**, 53-62 (2015).
686   19.   Villalba, R.M., Smith, Y. Loss and remodeling of striatal dendritic spines in Parkinson's
687   disease: from homeostasis to maladaptive plasticity? *Journal of Neural Transmission (Vienna).*
688   **125**, 431-447 (2018).
689   20.   Huerta-Ocampo, I., Mena-Segovia, J., Bolam, J.P. Convergence of cortical and thalamic
690   input to direct and indirect pathway medium spiny neurons in the striatum. *Brain Structure and*
691   *Function.* **219**, 1787-1800 (2014).
692   21.   Kincaid, A.E., Zheng, T., Wilson, C.J. Connectivity and convergence of single
693   corticostriatal axons. *Journal of Neuroscience.* **18**, 4722-4731 (1998).
694   22.   Reiner, A., Hart, N.M., Lei, W., Deng, Y. Corticostriatal projection neurons - dichotomous
695   types and dichotomous functions. *Frontiers in Neuroanatomy.* **4**, 142 (2010).
696   23.   Rothe, T. et al. Pathological gamma oscillations, impaired dopamine release, synapse
697   loss and reduced dynamic range of unitary glutamatergic synaptic transmission in the striatum
698   of hypokinetic Q175 Huntington mice. *Neuroscience.* **311**, 519-538 (2015) P.
699   24.   Dvorzhak, A., Helassa, N., Torok, K., Schmitz, D., Grantyn, R. Single synapse indicators of
700   impaired glutamate clearance derived from fast iGlu*u* imaging of cortical afferents in the
701   striatum of normal and Huntington (Q175) mice. *Journal of Neuroscience.* **39**, 3970-3982 (2019).
702   25.   Rebec, G.V. Corticostriatal network dysfunction in Huntington's disease: Deficits in
703   neural processing, glutamate transport, and ascorbate release. *CNS Neuroscience &*
704   *Therapeutics.* **10** (2018).

705 26.   Friedman, A. et al. Chronic Stress Alters Striosome-Circuit Dynamics, Leading to Aberrant
706 Decision-Making. *Cell.* **171**, 1191-1205 (2017).
707 27.   Helassa, N. et al. Ultrafast glutamate sensors resolve high-frequency release at Schaffer
708 collateral synapses. *Proceedings of the National Academy of Sciences of the United States of*
709 *America.* **115**, 5594-5599 (2018).
710 28.   Marvin, J.S. et al. An optimized fluorescent probe for visualizing glutamate
711 neurotransmission. *Nature Methods.* **10**, 162-170 (2013).
712 29.   Paxinos, G., Franklin, K.B.J. The Mouse Brain in Stereotaxic Coordinates. Elsevier (2003).
713 30.   Marcaggi, P., Attwell, D. Role of glial amino acid transporters in synaptic transmission
714 and brain energetics. *Glia.* **47**, 217-225 (2004).
715 31.   Bergles, D.E., Diamond, J.S., Jahr, C.E. Clearance of glutamate inside the synapse and
716 beyond. *Current Opinion in Neurobiology.* **9**, 293-298 (1999).
717 32.   Papouin, T., Dunphy, J., Tolman, M., Foley, J.C., Haydon, P.G. Astrocytic control of
718 synaptic function. *Philosophical Transactions of the Royal Society B: Biological Sciences.* **372**,
719 20160154 (2017).
720 33.   Tzingounis, A.V., Wadiche, J.I. Glutamate transporters: confining runaway excitation by
721 shaping synaptic transmission. *Nature Reviews Neuroscience.* **8**, 935-947 (2007).
722 34.   Nedergaard, M., Verkhratsky, A. Artifact versus reality--how astrocytes contribute to
723 synaptic events. *Glia.* 60, 1013-1023 (2012).
724 35.   Octeau, J.C., Faas, G., Mody, I., Khakh, B.S. Making, Testing, and Using Potassium Ion
725 Selective Microelectrodes in Tissue Slices of Adult Brain. *Journal of Visualized Experiments.* 10
726 (2018).
727 36.   Shrivastava, A.N., Aperia, A., Melki, R., Triller, A. Physico-Pathologic Mechanisms
728 Involved in Neurodegeneration: Misfolded Protein-Plasma Membrane Interactions. *Neuron.* **95**,
729 33-50 (2017).
730 37.   Langfelder, P. et al. Integrated genomics and proteomics define huntingtin CAG length-
731 dependent networks in mice. *Nature Neuroscience.* **19**, 623-633 (2016).
732 38.   Pal, B. Involvement of extrasynaptic glutamate in physiological and pathophysiological
733 changes of neuronal excitability. *Cellular and Molecular Life Sciences.* **75**, 2917-2949 (2018).
734 39.   Pekny, M. et al. Astrocytes: a central element in neurological diseases. *Acta*
735 *Neuropathologica.* **131**, 323-345 (2016).
736 40.   Bading H. Therapeutic targeting of the pathological triad of extrasynaptic NMDA
737 receptor signaling in neurodegenerations. *Journal of Experimental Medicine.* **214**, 569-578
738 (2017).
739 41.   Pajarillo, E., Rizor, A., Lee, J., Aschner, M., Lee, E. The role of astrocytic glutamate
740 transporters GLT-1 and GLAST in neurological disorders: Potential targets for
741 neurotherapeutics. *Neuropharmacology.* **10** (2019).
742 42.   Jensen, T.P., Zheng, K., Tyurikov,a O., Reynolds, J.P., Rusakov, D.A. Monitoring single-
743 synapse glutamate release and presynaptic calcium concentration in organised brain tissue. *Cell*
744 *Calcium.* **64**, 102-108 (2017).
745 43.   Reynolds, J.P., Zheng, K., Rusakov, D.A. Multiplexed calcium imaging of single-synapse
746 activity and astroglial responses in the intact brain. *Neuroscience Letters.* **10** (2018).
747 44.   Kuo, H.Y., Liu, F.C. Synaptic Wiring of Corticostriatal Circuits in Basal Ganglia: Insights
748 into the Pathogenesis of Neuropsychiatric Disorders. *eNeuro.* **6**, ENEURO-19 (2019).

749 45.   Untiet, V. et al. Glutamate transporter-associated anion channels adjust intracellular
750 chloride concentrations during glial maturation. *Glia.* **65**, 388-400 (2017).
751 46.   Burgold, J. et al. Cortical circuit alterations precede motor impairments in Huntington's
752 disease mice. *Scientific Reports.* **9**, 6634-43024 (2019).
753 47.   Jensen, T.P. et al. Multiplex imaging relates quantal glutamate release to presynaptic Ca
754 (2+) homeostasis at multiple synapses in situ. *Nature Communications.* **10**, 1414-09216 (2019).
755 48.   Inoue, M. et al. Rational Engineering of XCaMPs, a Multicolor GECI Suite for In Vivo
756 Imaging of Complex Brain Circuit Dynamics. *Cell.* **177**, 1346-1360 (2019).
757 49.   Durst, C.D. et al. High-speed imaging of glutamate release with genetically encoded
758 sensors. *Nature Protocols.* **14**, 1401-1424 (2019).
759
760

Figure2

Figure3

Figure4

Figure5

1 µm

−100   ΔF/F (%)   100

50 ΔF/F (%)

10 ms
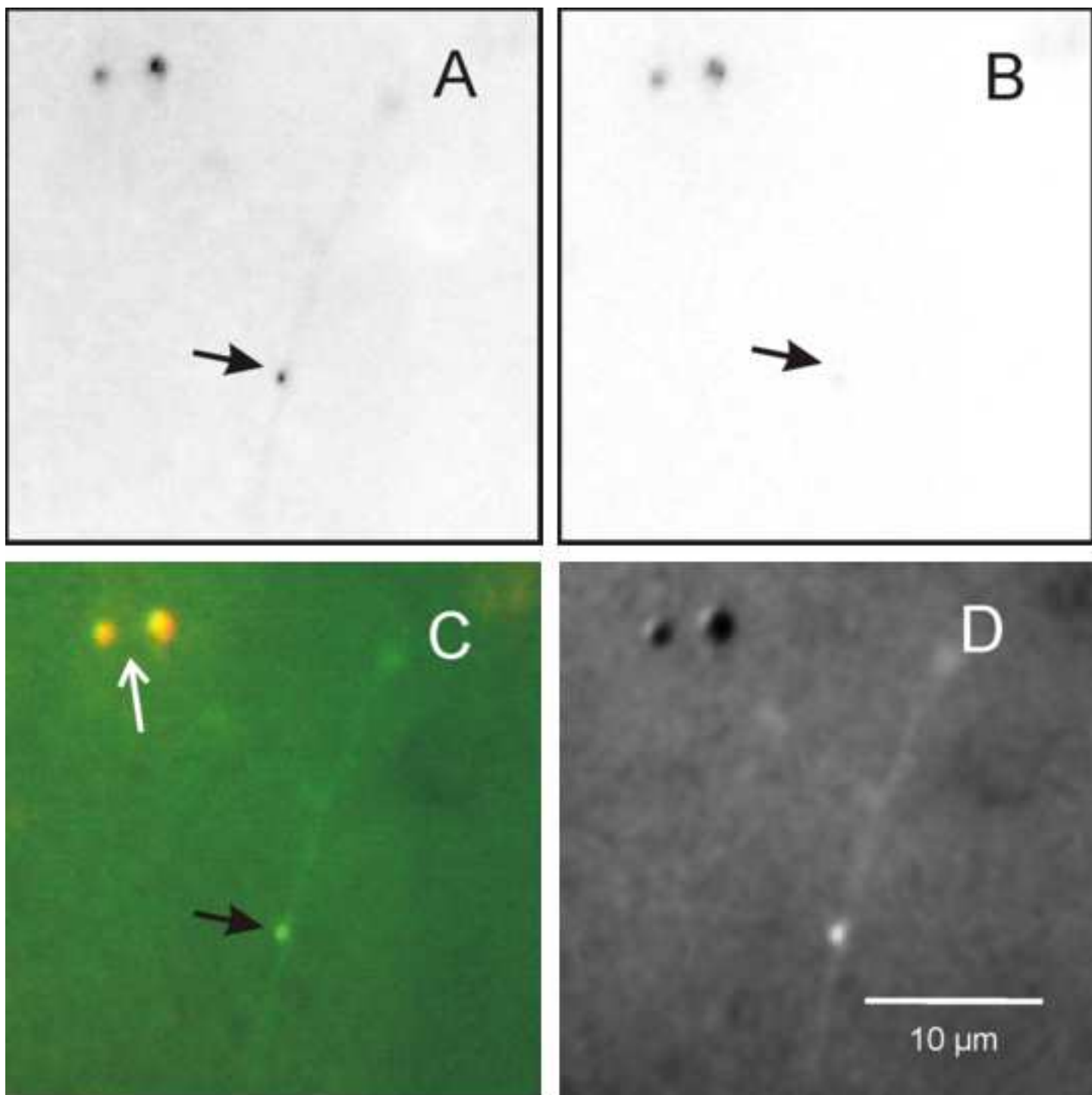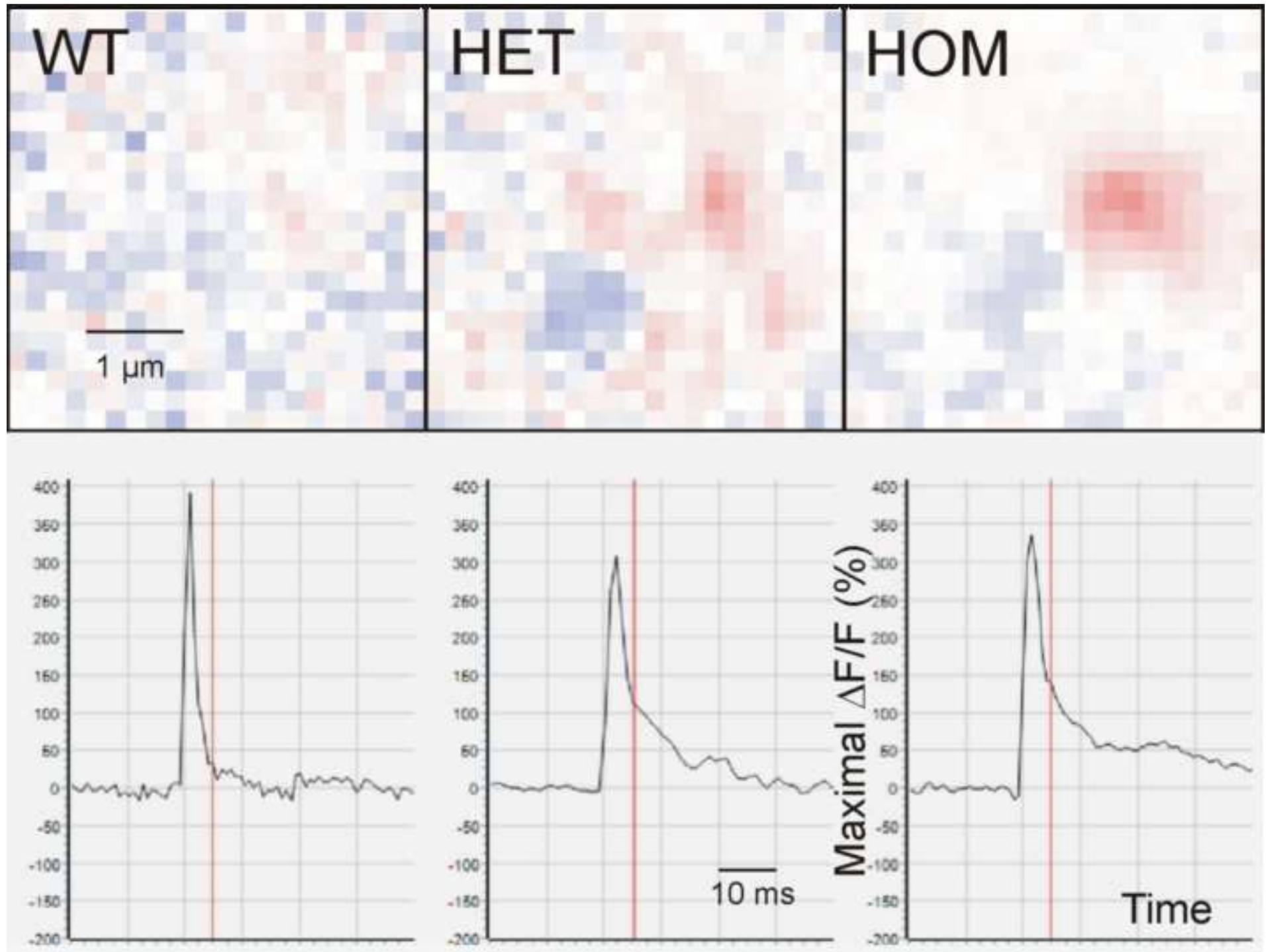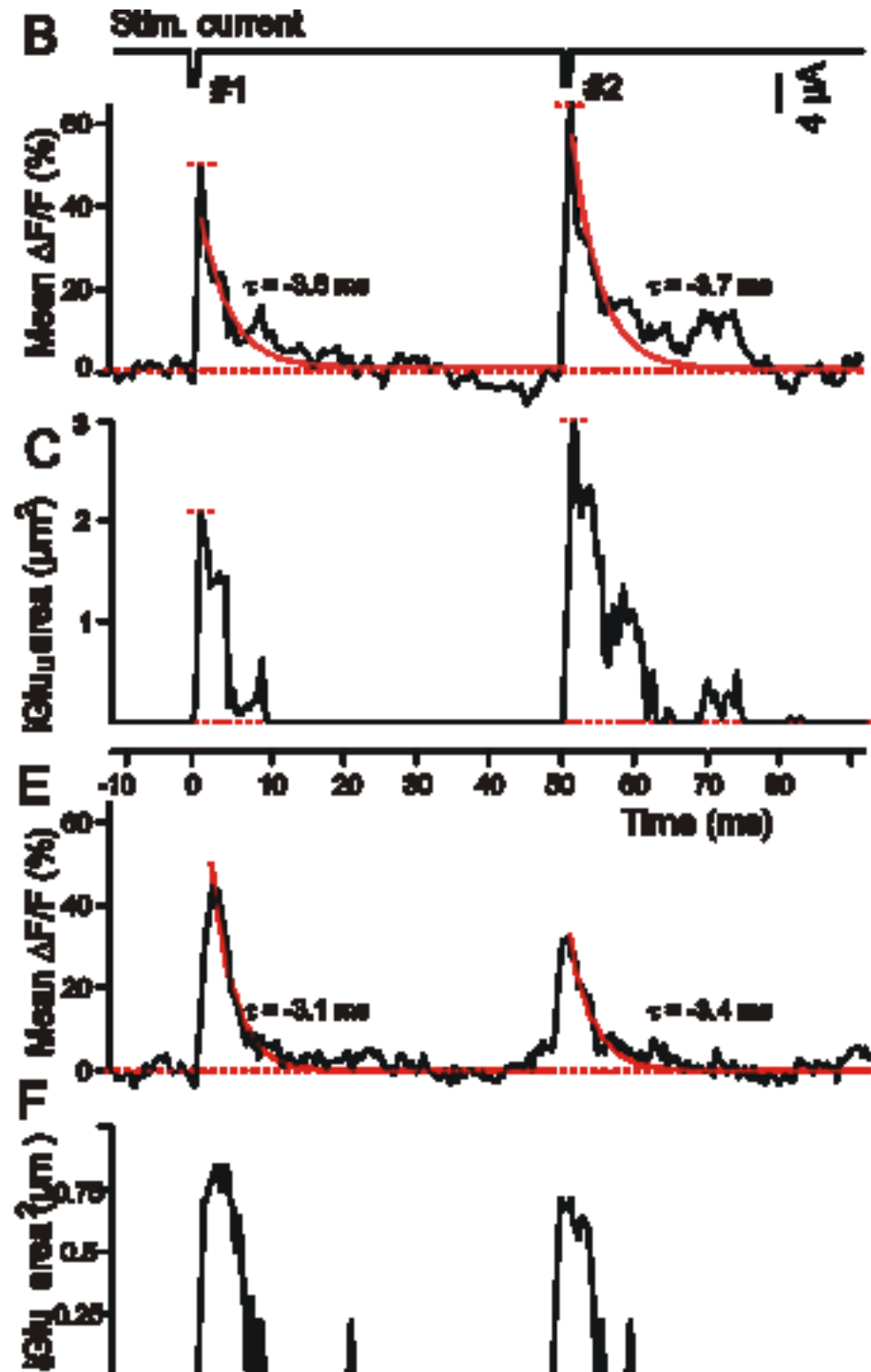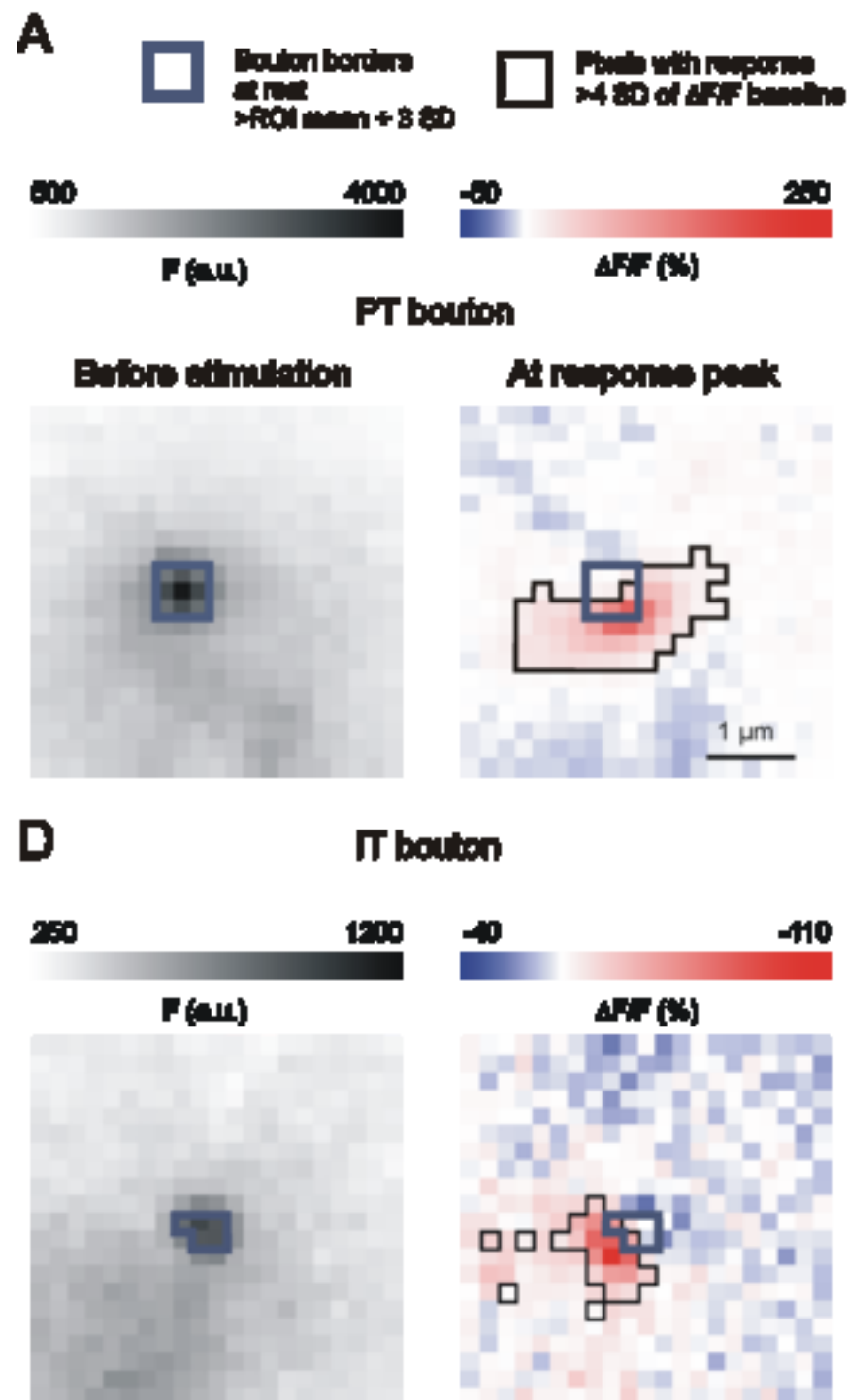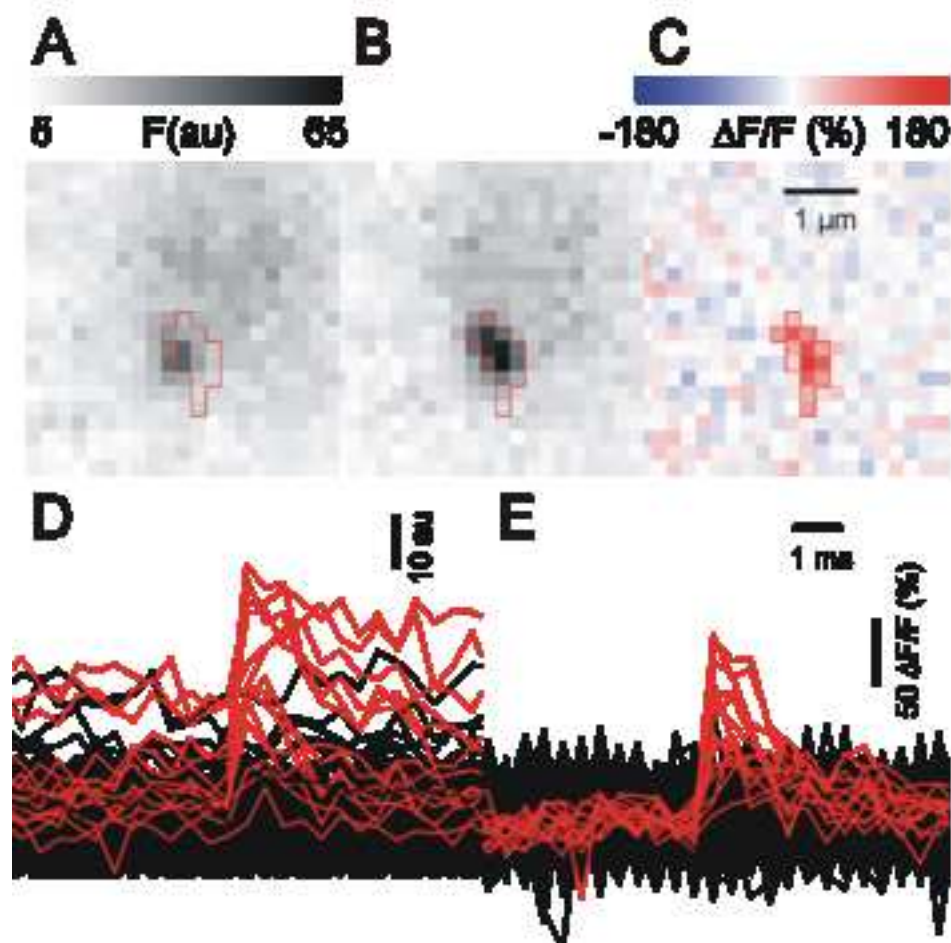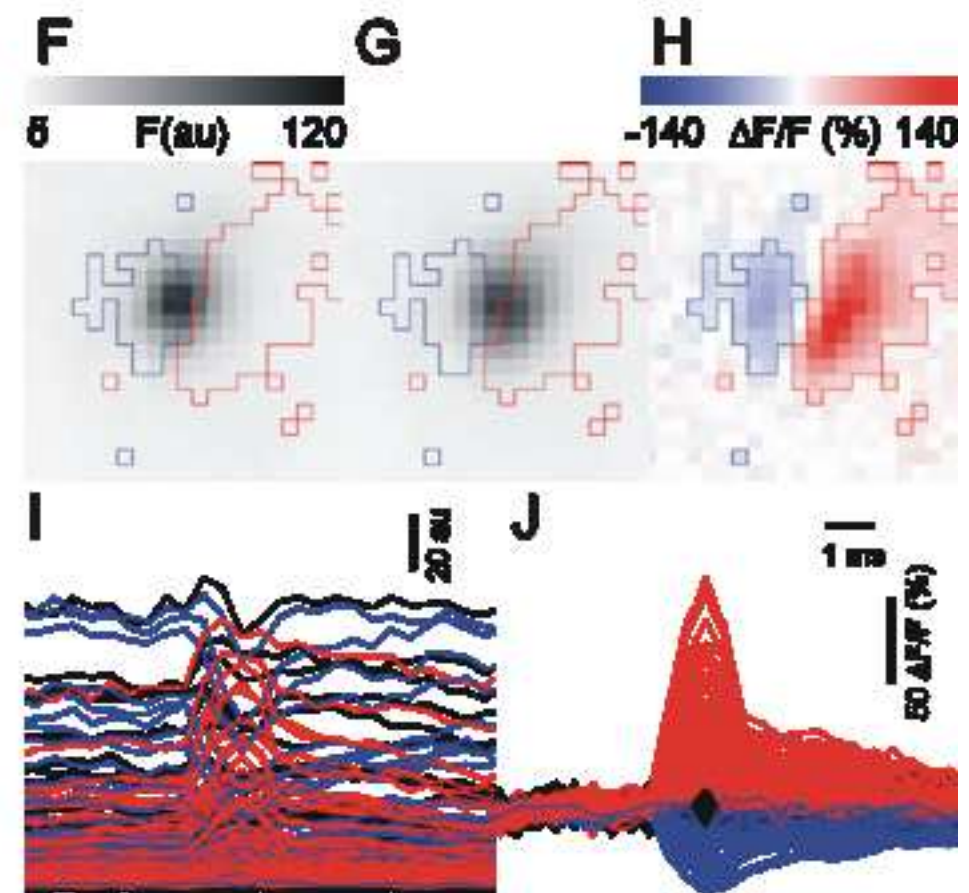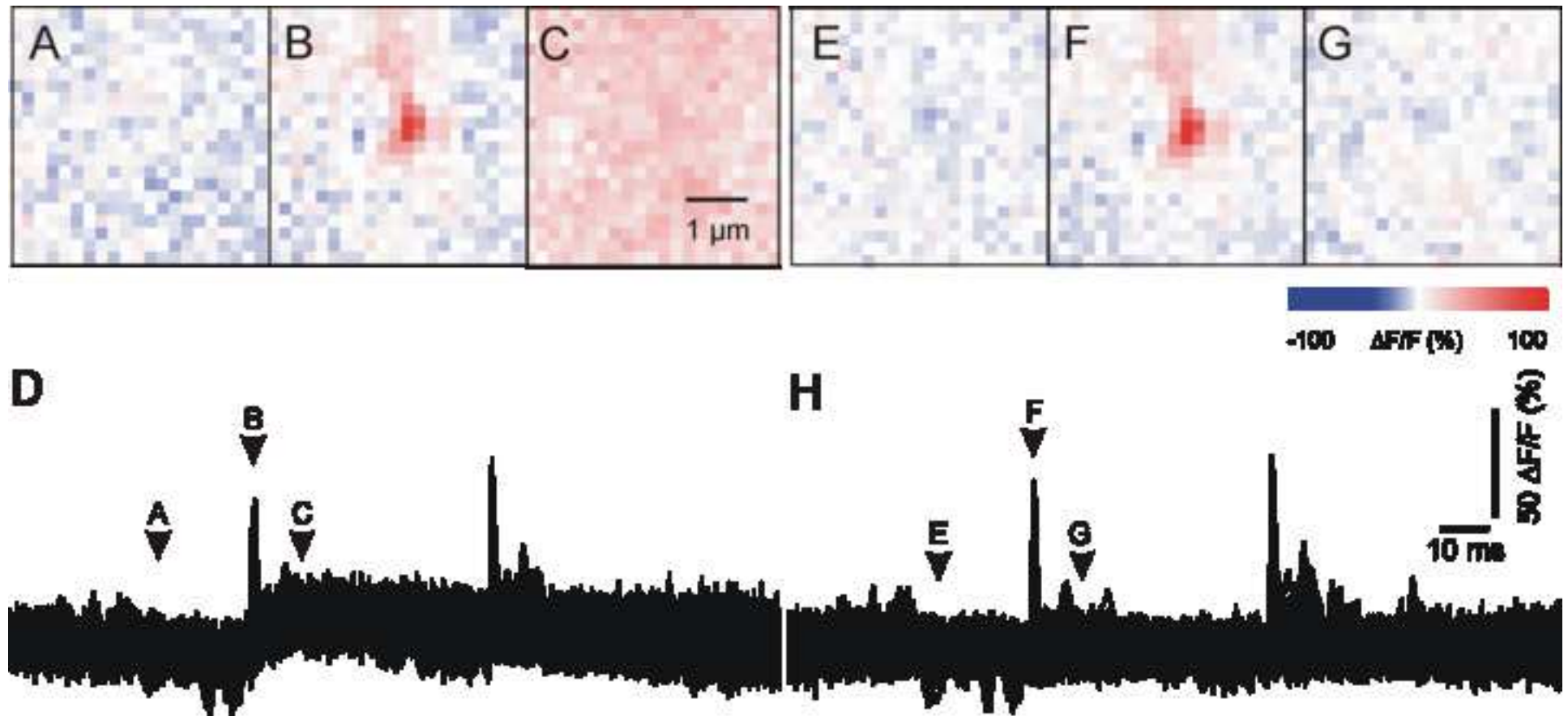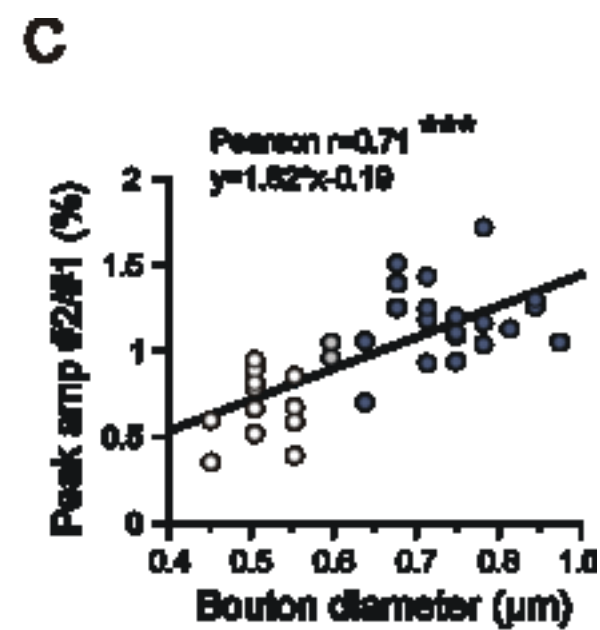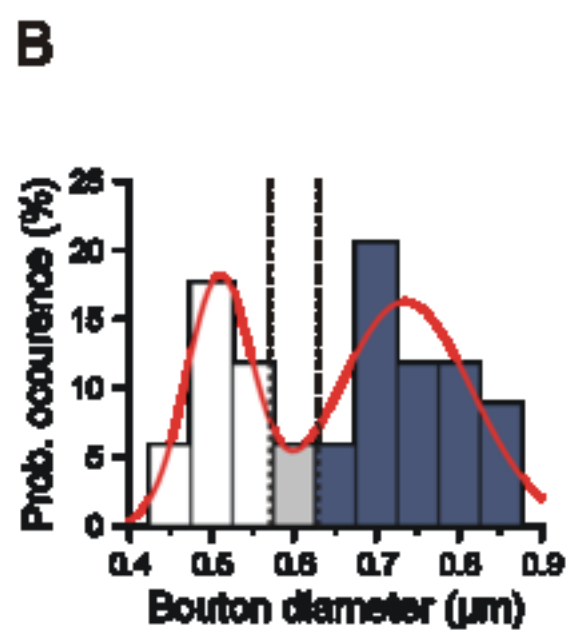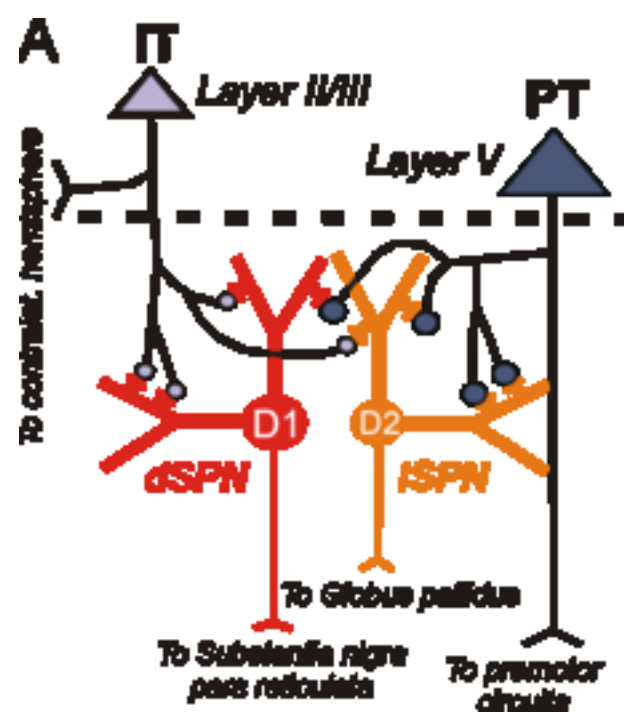
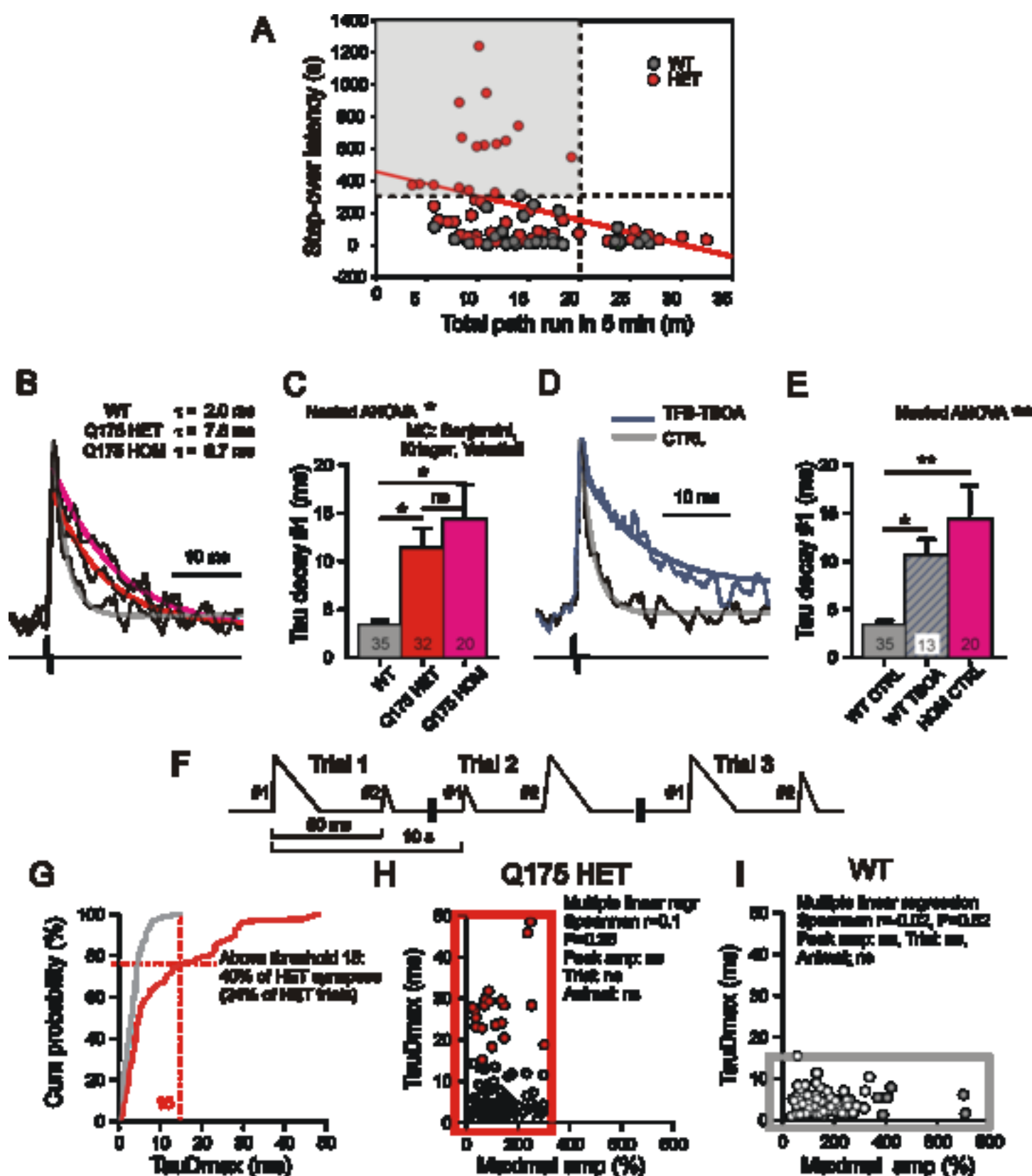Figure7

Click here to access/download

Video or Animated Figure
Q175_iGluSnFr-
ultrafast_WT_HET_HOM_2fps_(ALLConverter_1).mp4

Table1

Item/Purpose	Name	Company
Stereo microsope	Precision Stereo Zoom Binocular Microscope	WPI
Stereotaxic frame	Digital Lab New Standard stereotaxic frame	Stoelting
High speed drill equipment	Foredom K1070 cromoter Kit	Stoelting
Injection system	Quintessential Stereotaxic Injector (QSI)	Stoelting
Hamilton syringe 5 µl	75RN Syr (26s/51/2)	Hamilton
Laser positioning system	UGA-40	OptoElectronic
Blue laser for iGlu$u$ excitation	473 nm laser	OptoElectronic
Dichroic mirror for 473 nm	Dichroic	OptoElectronic
1P upright microscope	Axioskop 2 FS Plus	Carl Zeiss
Objective 63x/1.0	W Plan-Apochromat	Carl Zeiss
4x objective	Achroplan 4x/0,10	Carl Zeiss
Dichroic mirror for iGlu$u$		Omega optical
Emission filter for iGluu		Omega optical
Dichroic mirror		Omega optical
Emission filter for autofluorescence subtr.		Omega optical
sCMOS camera	ZYLA 4.2MP Plus	Andor
Acqustion software	Solis	Andor
AD/DA converter	InstruTECH LIH8+8	HEKA Elektronik
Aquisition software	TIDA5.25	HEKA Elektronik
Electrode positioning system	Micromanipulator	Sutter Instrument
Electrical stimulator		Charite workshops
Slicer	Vibrotome	Leica
Brown/Flaming-type puller	P-1000	Sutter Instr
Glass tubes for injection pipettes		WPI
Glass tubes forstimulation pipettes		WPI
Tetrodotoxin	TTX	Abcam
iGlu$u$ plasmid	pCI-syn-iGlu$_u$	Addgene
Q175 mice	Z-Q175-KI	Jackson Lab

Catalog Number
PZMIII
51500D
514439V
53311
87930
UGA-40
DL-473-020-S
473
000000-1066-600
421480-9900
44-00-20
XF2030
XF3086
QMAX_DI580LP
QMAX EM600-650
ZYLA4.2PCL10
4.30.30034.0
895035
895153
MPC-200
STIM-26
VT1200 S
SU-P1000
1B100F3
R100-F3
ab120054
106122
27410

Response to the Editor and the Reviewers

We are truly grateful to the Editor and the reviewers for the thorough attention to our manuscript. We have addressed all concerns. In the following the issues will be commented in the order of appearance in the reviews.

Dear Dr. Grantyn,

Editorial comments:
Changes to be made by the Author(s):
1. Please take this opportunity to thoroughly proofread the manuscript to ensure that there are no spelling or grammar issues. The JoVE editor will not copy-edit your manuscript and any errors in the submitted revision may be present in the published version. Please use American English throughout.
Done.

2. Please provide an email address for each author.
Done.

3. Please rephrase the Short Abstract/Summary to clearly describe the protocol and its applications in complete sentences between 10-50 words: "Here, we present a protocol to …"
Done.

4. Please remove all commercial language from your manuscript and use generic terms instead. All commercial products should be sufficiently referenced in the Table of Materials and Reagents.
For example: Andor Zyla4.2 plus sCMOS camera, Solis, version 4.30.30034.0 (Andor), Solis Control software (all from Rapp OptoElectronics), UGA-40, Rapp OptoElectronic, Andor Zyla4.2 plus, Zeiss 10 Axioskop 2 FS Plus, oftware TIDA 5.24 (both HEKA 28 Elektronik), etc.
Done, see attached Table 1.

5. Please adjust the numbering of the Protocol to follow the JoVE Instructions for Authors. For example, 1 should be followed by 1.1 and then 1.1.1 and 1.1.2 if necessary. Please refrain from using bullets or dashes.
Done.

6. Please revise the protocol text to avoid the use of any personal pronouns in the protocol (e.g., "we", "you", "our" etc.).
Done.

7. Please ensure that all text in the protocol section is written in the imperative tense as if telling someone how to do the technique (e.g., "Do this," "Ensure that," etc.). The actions should be described in the imperative tense in complete sentences wherever possible. Avoid usage of phrases such as "could be," "should be," and "would be" throughout the Protocol. Any text that cannot be written in the imperative tense may be added as a "Note."
Done.

8. The Protocol should contain only action items that direct the reader to do something. Please move the discussion about the protocol to the Discussion.

Done. See addition to Discussion on page 14.

9. The Protocol should be made up almost entirely of discrete steps without large paragraphs of text between sections. Please ensure that individual steps of the protocol should only contain 2-3 actions per step.

Done.

10. Please add more details to your protocol steps. Please ensure you answer the "how" question, i.e., how is the step performed?

Done.

11. Software steps must be more explicitly explained ('click', 'select', etc.). Please add more specific details (e.g. button clicks for software actions, numerical values for settings, etc.).

12. 1.4: How do you check the depth of anesthesia? How do you sterilize the site of surgery? Do you shave the surgical site?

13. 1.6: How is this done?

14. 2.1: Please make action steps in imperative tense using complete sentences.

15. 2.2, Note: Some of the details of this note can be moved to the discussion.

16. 2.2.1: How were the slices made?

17. 3: Please write in action steps only, discussion about the action can be included in the discussion section.

18. 3.2.1: We cannot have paragraph of texts in the protocol section, please make substeps instead.

19. 3.3: Please include how do you perform each step.

Changed as requested.

20. There is a 10-page limit for the Protocol, but there is a 2.75-page limit for filmable content. Please highlight 2.75 pages or less of the Protocol (including headings and spacing) that identifies the essential steps of the protocol for the video, i.e., the steps that should be visualized to tell the most cohesive story of the Protocol.

The 2.7 pages are highlighted in azure.

21. Please obtain explicit copyright permission to reuse any figures from a previous publication. Explicit permission can be expressed in the form of a letter from the editor or a link to the editorial policy that allows re-prints. Please upload this information as a .doc or .docx file to your Editorial Manager account. The Figure must be cited appropriately in the Figure Legend, i.e. "This figure has been modified from [citation]."

Done. The permission to reproduce Figures published in The Journal of Neuroscience will be forwarded to the Editorial manager of JOVE.

22. As we are a methods journal, please revise the Discussion to explicitly cover the following in detail in 3-6 paragraphs with citations:
a) Critical steps within the protocol
b) Any modifications and troubleshooting of the technique

c) Any limitations of the technique
d) The significance with respect to existing methods
e) Any future applications of the technique.
We have added respective text to the Discussion.

23. Please include all the Figure Legends together at the end of the Representative Results in the manuscript text. Please remove the legends from the figure.
Done.

24. Please include a table of the essential supplies, reagents, and equipment. The table should include the name, company, and catalog number of all relevant materials in separate columns in an xls/xlsx file.
Done.

25: Please reword lines 23-32 in the introduction section and 2.2. note: first sentence as it matches with previously published literatures.
Done.

<u>**Reviewer #1:**</u>

The description of the surgery and a detailed list of reagents and materials is lacking (glass pipettes, drugs, etc), but this can be easily fixed.
Is now added.

I also am asking that figure 6 include raw data of the PPR experiments, not just the summary graphs!
The requested original traces from PT/IT synapses for the summary graphs of Fig. 6 are now added to Fig. 3. A respective reference is included in the text and the legend to Fig. 6.

Why can't regular epifluorescence be used? why only a scanning laser? or am I missing something? please clarify.
It's the balance between sufficient excitation and bleaching. Focal illumination protects the fluorescence out of the region of interest. The use of a focal 1P laser places the present approach somewhere between regular epifluorescence and 2PLSM. It is the method of choice if the signal obtained with a genetically encoded glutamate indicator (GEGI) at rest is too low for detection with 2P optics.

How do you take the optical resolution limit into consideration (I'd imagine you should never have more than 5 pixels per micron)?
With the 63x objective and the Andor Zyla one may have 10 pixels per μm. It is possible to work with such resolution, but our recommendation is to work with binning 2x2.

Can you please discuss the prospects of this becoming and in vivo (e.g., 2PLSM) technique?
We have mentioned in the Discussion that the present approach can be applied to in vivo brain preparations. To explain more details would be a topic for another JoVE paper. Off-line: Single

synapse imaging in intact mice is certainly possible with genetically encoded Ca sensors (Reynolds et al 2018). We hope that the addition of Ca imaging (and illumination with a second laser) will facilitate the search of presynaptic varicosities expressing a fast GEGI. Using the present approach (without a Ca indicator) we have performed *in vivo* recordings from the contralateral premotor cortex. At this point we can already say that iGlu*u* imaging of single glutamatergic terminals appears to be feasible in the superficial layers of the (motor) cortex of anesthetized mice. A 2PLSM has now become available as well, but the experiments are only starting. At this point we can only refer to the exquisite method description of Dürst et al in Nat Prot 2019 who describe experiments in cultures from neonatal hippocampi. However, after becoming aware of the influence of astrocytes on glutamatergic synaptic transmission cultures are not that attractive. All further efforts should go towards single synapse imaging in the intact brain.

p1 l16 - missing space in A25%
Corrected.

p1 l17 - remains no remain
Corrected

p2 l12 - Because not Since
Corrected

p3 l4 missing space in proper name
Corrected

p3 l23 are these adenoviruses or adenoassociated viruses as mentioned below (e.g., l 31)?
Corrected

p3 l 29 do you need to cut the pipette tips after the pull? please say something about the pulling parameters (e.g., is it a single pull?). Also, the exact kind of glass you use (OD, ID and including supplier) should be mentioned. Also what puller (supplier) do you use?
Text added.

p3 l32 are you sure you do not maintain your viruses on ice until the actual injection? why do you leave it at RT?
We rely on experiments of the Charité viral core facility technicians who specifically investigated this issue. Their recommendation is to avoid any freezing of virus preps if they are used within the next 6 months. After virus production we keep part of the virus at 5 $^{\circ}$C and take the respective tube out of the fridge just before the mouse is anesthetized. The other part is aliquoted and stored at -80 $^{\circ}$C. In that case we do not use ice till the final use after unfreezing. Here we report a working protocol, but cannot discuss the pros and cons of virus storage recommendations.

p3 l37 what stereotaxic frame did you use? (supplier)
Added to Table 1.

p4 l1 what about shaving hairs and sterilization with alcohol and/or betadyne?

Added to Text.

p4 l2 - do you inject manually or with an injection system? Please explain how you monitor the injection rate. Details of how you mount the pipette would also help (i.e., is there use of oil for a pneumatic effect?)
Added to Text.

p4 l4 guarantees instead of secures
Corrected.

p5 l10 what stimulator did you use?
Added to Table 1.

p5 l21 please say which objective you used (Zeiss?).
Added to Table 1.

p 6 ll12-14 Please discuss how imaging would be done in conjunction with optogenetics (eg., issue of wavelengths etc). I can foresee two issues: 1. accidentally activating the opsin; and 2. bleaching the fluorescence while activating opsins with light. (btw channelrhodopsin should be without a space).
The use of channelrhodopsin can well be combined with single bouton iGlu*u* imaging if the former is activated by focal stimulation at a distant site, e.g. the contralateral cortex. In the described experiments we stimulate close to the monitored varicosity and therefore refrained from the use of channelrhodopsins. The text has now been changed in accordance.

p 6 l17 please explain above how you pull the stim electrode? what about using theta class or a metal electrode? please discuss.
Done.

p 6 l 22 what concentration of TTX would you use?
Done.

p 9 l 6 how can you be sure that the explanation is that the other terminals do not express the iGluu, perhaps they do but they are simply outside the FoV or depth of field so that you don't see them clearly. I think that is just as likely an explanation as the other fibers not expressing the iGluu. In fact, if you have a spurious signal doesn't that mean that it must be from terminals the DO express iGluu? please explain.
That paragraph needed a complete re-writing, we agree. See new version on p9 ll23-29.

p 9 l 19 change als to also
Done.

p10 l 11 and not andf
Done.

p 10 l 22 missing space in TauDwas

Done.

fig. 4 caption. not clear what is meant by "the brightest pixels at rest are moved". what does "moved" mean in this context?
Text changed to make the point clearer. See p11, ll41-42.

At first sight figure7E, right (HOM) is misleading - it looks as large an effect as on the left (wt) but you say that it's not significant. Are you sure there isn't a trend? Although, I can't imagine how TBOA could shorten TauD in homozygous Q175s? in any event, if it's not significant, please stress this in the figure legend.
Yes, we agree. We have now removed the confusing results from the TBOA experiments in HOM altogether.

Reviewer #2:

1) The dissociation constant for iGluu is mention to be 2.1 ms (page 3). Glutamate Tau decay in WT slices amounts to about 2.0 ms (Fig. 7).
We have made changes on p3 ll9-13 to make this point more clear. The off-rate of 2.1 ms in the Helassa et al 2018 paper refers to their experiments in a stopped-flow device at a temperature of 20 $^{\circ}$C. The extrapolated value for 34 $^{\circ}$C was 0.68 ms. It can therefore be assumed that the decay time constant of the iGlu fluorescence is determined by diffusion and uptake rather than the kinetic characteristics of the sensor. The mean TauD on WT was 3.4 ms. The example chosen in Fig. 7 is probably one with a particularly fast decay, but still longer than the 0.68 ms estimated for the sensor by Helassa et al 2018.

Does a two-exponential fit provide better approximation?
No.

2) The authors refer to astrocyte-mediated glutamate clearance in all parts of the manuscript and show the TFB-TBOA-induced changes data (Fig.7 E). However prolongation of Tau decay might be a result of reduced number of EAATs and/or altering of astrocyte morphology (and, as a result, change of diffusion rate). It is very difficult to separate these changes, but the authors could discuss this point when writing about "glutamate spread" (Fig. 3)?
We admit that the use of the term "clearance" in synaptic physiology is somewhat ambiguous. In general pharmacology and in renal physiology, "the clearance is a pharmacokinetic measurement of the volume of plasma from which a substance is completely removed per unit time; the usual units are mL/min." In most cases this is a virtual indicator. As we do not have exact estimates of the involved volumes, any change in the glutamate concentration (iGlu$_u$ fluorescence) next to the releasing terminal may as well reflect a change both in uptake and in volume of perisynaptic space. But the lack of disease related difference in the "*Spread Velocity*" (Dvorzhak et al 2019, Fig. 4M). argues against a change in volume/diffusion. Furthermore, a genetically induced recovery of astrocytic uptake EAAT2 function (Hirschberg, Dvorzhak et al, unpublished) resulted in complete

recovery of iGlu$_u$ TauD. We therefore believe that in the P-type corticostriatal synapses glutamate clearance is indeed strongly determined by the rate of glutamate uptake.

To illuminate the complex interrelationships between glutamate uptake and clearance would require qualified modeling and should be subject of a more theoretical paper. For the present communication we prefer to limit ourselves to what is said in the present text, but see the additions on p10, ll33-42.

3) page 7, lines 38-40 "8) … Note: After 10 trials, iGluu is fully bleached. The maximal illumination time with the 1 photon laser system and the described setting is approximately 2 s." Is the bleaching linear? As the peak amplitude of iGluu probe is proposed to reflect the near-synaptic glutamate concentration, the question arises whether the bleaching would distort the signal. Please discuss.
This is one of the most critical aspects of the method. We have added some text to underline what the method in its present implementation can give or not (p14, ll10-31).

Fig. 6 shows the paired-pulse plasticity at distinct synaptic varicosities. AP-induced glutamate release has a probabilistic nature, i.e. to obtain a representative paired-pulse ratio, several trials have to be applied. Values in Panel C represent values derived from how many trials?
The values in panel C represent the averages of from the first 3 trials in each tested bouton. This information has now been added to the legend.

1) Abstract "..single synapse resolution can be achieved in fully mature acute brain slices.." What is a fully mature slice? Please rephrase.
Done.

2) page 3, line 1-3 "Here we describe a new approach which allows one to 1 evaluate single synapse glutamate clearance in its relation to the amount of the released neurotransmitter after expression of the genetically encoded glutamate sensor IGluu in the presynaptic plasma membrane." This sentence sounds as if the release would be dependent on the IGluu expression. Please rewrite.
Done.

3) page 4, line 2 "Place the pipette in the cortex…" At which angle?
Done.

4) page 5, top „….[Glu] levels below 100 nM. Accordingly, any sensor of glutamate, and especially a low affinity sensor like iGluu will be rather dim in the absence of synaptic glutamate release." Is there any fluorescent signal from iGluu at resting conditions?
Yes. See Fig. 3 "Before stimulation" and Chapter 2.2.

Fig. 3B shows that F0 is about 500 a.u. Is this a representative value? How strong (in a.u.) is the background fluorescent after the suggested correction.
This is a representative value. After subtraction of autofluorescence the mean background fluorescence F is typically 400-700 a.u. See new text p6 l17.

5) page 9, line 10. "It als decays more slowly". Please correct.
Done.

Betreff:
[ext] Re: Permit to reproduce modified versions of Figures published in The Journal of Neuroscience
Von:
JN_EiC <jn_eic@sfn.org>
Datum:
14.05.2019, 19:01
An:
grantyn <rosemarie.grantyn@charite.de>

Dear Dr. Grantyn,

JNeuroscience authors retain full copyright to their work. You are free to use the figures in your recent paper as you wish, as long as you provide full attribution to the JNeuroscience paper in which they appear.

Yours,

Marina Picciotto
Editor in Chief
The Journal of Neuroscience

On May 14, 2019, at 12:59 PM, grantyn <rosemarie.grantyn@charite.de> wrote:

> Dear Dr. Picciotto,
>
> Anton Dvorzhak and I are preparing a Methods paper for JoVE where we would like to illustrate Representative Results from our recent publication in The Journal of Neuroscience (PMID: 30819797). This will be modified figures from the original Figs. 1B,C,D,E,H, 4D,E,G,I,5A,G,H,I and the Movie1 Still. If possible we would also reproduce the Movie itself.
>
> The permit can be expressed as a letter from the Editor.
>
> Thank you very much for your attention to our request.
>
> With best regards,
>
> Rosemarie Grantyn
>
>
> --
> Prof. Dr. med. Rosemarie Grantyn
> Charité - Universitätsmedizin (CCM)
> Neurowissenschaftliches Forschungszentrum (NWFZ)
> Robert-Koch-Platz 4, 3. Ebene, Raum 027 o. 004
> Fon: 450528165 (David Betances)
> <rosemarie_grantyn.vcf>

jove
JOURNAL OF
VISUALIZED EXPERIMENTS

1 Alewife Center #200
Cambridge, MA 02140
tel. 617.945.9051
www.jove.com

ARTICLE AND VIDEO LICENSE AGREEMENT

Title of Article:	Single synapse indicators of glutamate release and uptake in acute brain slices from normal and Huntington mice
Author(s):	Anton Dvorzhak and Rosemarie Grantyn

Item 1: The Author elects to have the Materials be made available (as described at http://www.jove.com/publish) via:

[X] Standard Access   [ ] Open Access

Item 2: Please select one of the following items:

[X] The Author is **NOT** a United States government employee.

[ ] The Author is a United States government employee and the Materials were prepared in the course of his or her duties as a United States government employee.

[ ] The Author is a United States government employee but the Materials were NOT prepared in the course of his or her duties as a United States government employee.

ARTICLE AND VIDEO LICENSE AGREEMENT

1. **Defined Terms.** As used in this Article and Video License Agreement, the following terms shall have the following meanings: "**Agreement**" means this Article and Video License Agreement; "**Article**" means the article specified on the last page of this Agreement, including any associated materials such as texts, figures, tables, artwork, abstracts, or summaries contained therein; "**Author**" means the author who is a signatory to this Agreement; "**Collective Work**" means a work, such as a periodical issue, anthology or encyclopedia, in which the Materials in their entirety in unmodified form, along with a number of other contributions, constituting separate and independent works in themselves, are assembled into a collective whole; "**CRC License**" means the Creative Commons Attribution-Non Commercial-No Derivs 3.0 Unported Agreement, the terms and conditions of which can be found at: http://creativecommons.org/licenses/by-nc-nd/3.0/legalcode; "**Derivative Work**" means a work based upon the Materials or upon the Materials and other pre-existing works, such as a translation, musical arrangement, dramatization, fictionalization, motion picture version, sound recording, art reproduction, abridgment, condensation, or any other form in which the Materials may be recast, transformed, or adapted; "**Institution**" means the institution, listed on the last page of this Agreement, by which the Author was employed at the time of the creation of the Materials; "**JoVE**" means MyJove Corporation, a Massachusetts corporation and the publisher of The Journal of Visualized Experiments; "**Materials**" means the Article and / or the Video; "**Parties**" means the Author and JoVE; "**Video**" means any video(s) made by the Author, alone or in conjunction with any other parties, or by JoVE or its affiliates or agents, individually or in collaboration with the Author or any other parties, incorporating all or any portion of the Article, and in which the Author may or may not appear.

2. **Background.** The Author, who is the author of the Article, in order to ensure the dissemination and protection of the Article, desires to have the JoVE publish the Article and create and transmit videos based on the Article. In furtherance of such goals, the Parties desire to memorialize in this Agreement the respective rights of each Party in and to the Article and the Video.

3. **Grant of Rights in Article.** In consideration of JoVE agreeing to publish the Article, the Author hereby grants to JoVE, subject to **Sections 4** and **7** below, the exclusive, royalty-free, perpetual (for the full term of copyright in the Article, including any extensions thereto) license (a) to publish, reproduce, distribute, display and store the Article in all forms, formats and media whether now known or hereafter developed (including without limitation in print, digital and electronic form) throughout the world, (b) to translate the Article into other languages, create adaptations, summaries or extracts of the Article or other Derivative Works (including, without limitation, the Video) or Collective Works based on all or any portion of the Article and exercise all of the rights set forth in (a) above in such translations, adaptations, summaries, extracts, Derivative Works or Collective Works and (c) to license others to do any or all of the above. The foregoing rights may be exercised in all media and formats, whether now known or hereafter devised, and include the right to make such modifications as are technically necessary to exercise the rights in other media and formats. If the "Open Access" box has been checked in **Item 1** above, JoVE and the Author hereby grant to the public all such rights in the Article as provided in, but subject to all limitations and requirements set forth in, the CRC License.

612542.6   For questions, please contact us at submissions@jove.com or +1.617.945.9051.

jove
JOURNAL OF
VISUALIZED EXPERIMENTS

1 Alewife Center #200
Cambridge, MA 02140
tel. 617.945.9051
www.jove.com

ARTICLE AND VIDEO LICENSE AGREEMENT

4.   **Retention of Rights in Article.** Notwithstanding the exclusive license granted to JoVE in **Section 3** above, the Author shall, with respect to the Article, retain the non-exclusive right to use all or part of the Article for the non-commercial purpose of giving lectures, presentations or teaching classes, and to post a copy of the Article on the Institution's website or the Author's personal website, in each case provided that a link to the Article on the JoVE website is provided and notice of JoVE's copyright in the Article is included. All non-copyright intellectual property rights in and to the Article, such as patent rights, shall remain with the Author.

5.   **Grant of Rights in Video – Standard Access.** This **Section 5** applies if the "Standard Access" box has been checked in **Item 1** above or if no box has been checked in **Item 1** above. In consideration of JoVE agreeing to produce, display or otherwise assist with the Video, the Author hereby acknowledges and agrees that, Subject to **Section 7** below, JoVE is and shall be the sole and exclusive owner of all rights of any nature, including, without limitation, all copyrights, in and to the Video. To the extent that, by law, the Author is deemed, now or at any time in the future, to have any rights of any nature in or to the Video, the Author hereby disclaims all such rights and transfers all such rights to JoVE.

6.   **Grant of Rights in Video – Open Access.** This **Section 6** applies only if the "Open Access" box has been checked in **Item 1** above. In consideration of JoVE agreeing to produce, display or otherwise assist with the Video, the Author hereby grants to JoVE, subject to **Section 7** below, the exclusive, royalty-free, perpetual (for the full term of copyright in the Article, including any extensions thereto) license (a) to publish, reproduce, distribute, display and store the Video in all forms, formats and media whether now known or hereafter developed (including without limitation in print, digital and electronic form) throughout the world, (b) to translate the Video into other languages, create adaptations, summaries or extracts of the Video or other Derivative Works or Collective Works based on all or any portion of the Video and exercise all of the rights set forth in (a) above in such translations, adaptations, summaries, extracts, Derivative Works or Collective Works and (c) to license others to do any or all of the above. The foregoing rights may be exercised in all media and formats, whether now known or hereafter devised, and include the right to make such modifications as are technically necessary to exercise the rights in other media and formats. For any Video to which this **Section 6** is applicable, JoVE and the Author hereby grant to the public all such rights in the Video as provided in, but subject to all limitations and requirements set forth in, the CRC License.

7.   **Government Employees.** If the Author is a United States government employee and the Article was prepared in the course of his or her duties as a United States government employee, as indicated in **Item 2** above, and any of the licenses or grants granted by the Author hereunder exceed the scope of the 17 U.S.C. 403, then the rights granted hereunder shall be limited to the maximum

rights permitted under such statute. In such case, all provisions contained herein that are not in conflict with such statute shall remain in full force and effect, and all provisions contained herein that do so conflict shall be deemed to be amended so as to provide to JoVE the maximum rights permissible within such statute.

8.   **Protection of the Work.** The Author(s) authorize JoVE to take steps in the Author(s) name and on their behalf if JoVE believes some third party could be infringing or might infringe the copyright of either the Author's Article and/or Video.

9.   **Likeness, Privacy, Personality.** The Author hereby grants JoVE the right to use the Author's name, voice, likeness, picture, photograph, image, biography and performance in any way, commercial or otherwise, in connection with the Materials and the sale, promotion and distribution thereof. The Author hereby waives any and all rights he or she may have, relating to his or her appearance in the Video or otherwise relating to the Materials, under all applicable privacy, likeness, personality or similar laws.

10.   **Author Warranties.** The Author represents and warrants that the Article is original, that it has not been published, that the copyright interest is owned by the Author (or, if more than one author is listed at the beginning of this Agreement, by such authors collectively) and has not been assigned, licensed, or otherwise transferred to any other party. The Author represents and warrants that the author(s) listed at the top of this Agreement are the only authors of the Materials. If more than one author is listed at the top of this Agreement and if any such author has not entered into a separate Article and Video License Agreement with JoVE relating to the Materials, the Author represents and warrants that the Author has been authorized by each of the other such authors to execute this Agreement on his or her behalf and to bind him or her with respect to the terms of this Agreement as if each of them had been a party hereto as an Author. The Author warrants that the use, reproduction, distribution, public or private performance or display, and/or modification of all or any portion of the Materials does not and will not violate, infringe and/or misappropriate the patent, trademark, intellectual property or other rights of any third party. The Author represents and warrants that it has and will continue to comply with all government, institutional and other regulations, including, without limitation all institutional, laboratory, hospital, ethical, human and animal treatment, privacy, and all other rules, regulations, laws, procedures or guidelines, applicable to the Materials, and that all research involving human and animal subjects has been approved by the Author's relevant institutional review board.

11.   **JoVE Discretion.** If the Author requests the assistance of JoVE in producing the Video in the Author's facility, the Author shall ensure that the presence of JoVE employees, agents or independent contractors is in accordance with the relevant regulations of the Author's institution. If more than one author is listed at the beginning of this Agreement, JoVE may, in its sole

discretion, elect not take any action with respect to the Article until such time as it has received complete, executed Article and Video License Agreements from each such author. JoVE reserves the right, in its absolute and sole discretion and without giving any reason therefore, to accept or decline any work submitted to JoVE. JoVE and its employees, agents and independent contractors shall have full, unfettered access to the facilities of the Author or of the Author's institution as necessary to make the Video, whether actually published or not. JoVE has sole discretion as to the method of making and publishing the Materials, including, without limitation, to all decisions regarding editing, lighting, filming, timing of publication, if any, length, quality, content and the like.

12. **Indemnification.** The Author agrees to indemnify JoVE and/or its successors and assigns from and against any and all claims, costs, and expenses, including attorney's fees, arising out of any breach of any warranty or other representations contained herein. The Author further agrees to indemnify and hold harmless JoVE from and against any and all claims, costs, and expenses, including attorney's fees, resulting from the breach by the Author of any representation or warranty contained herein or from allegations or instances of violation of intellectual property rights, damage to the Author's or the Author's institution's facilities, fraud, libel, defamation, research, equipment, experiments, property damage, personal injury, violations of institutional, laboratory, hospital, ethical, human and animal treatment, privacy or other rules, regulations, laws, procedures or guidelines, liabilities and other losses or damages related in any way to the submission of work to JoVE, making of videos by JoVE, or publication in JoVE or elsewhere by JoVE. The Author shall be responsible for, and shall hold JoVE harmless from, damages caused by lack of sterilization, lack of cleanliness or by contamination due to

the making of a video by JoVE its employees, agents or independent contractors. All sterilization, cleanliness or decontamination procedures shall be solely the responsibility of the Author and shall be undertaken at the Author's expense. All indemnifications provided herein shall include JoVE's attorney's fees and costs related to said losses or damages. Such indemnification and holding harmless shall include such losses or damages incurred by, or in connection with, acts or omissions of JoVE, its employees, agents or independent contractors.

13. **Fees.** To cover the cost incurred for publication, JoVE must receive payment before production and publication the Materials. Payment is due in 21 days of invoice. Should the Materials not be published due to an editorial or production decision, these funds will be returned to the Author. Withdrawal by the Author of any submitted Materials after final peer review approval will result in a US$1,200 fee to cover pre-production expenses incurred by JoVE. If payment is not received by the completion of filming, production and publication of the Materials will be suspended until payment is received.

14. **Transfer, Governing Law.** This Agreement may be assigned by JoVE and shall inure to the benefits of any of JoVE's successors and assignees. This Agreement shall be governed and construed by the internal laws of the Commonwealth of Massachusetts without giving effect to any conflict of law provision thereunder. This Agreement may be executed in counterparts, each of which shall be deemed an original, but all of which together shall be deemed to me one and the same agreement. A signed copy of this Agreement delivered by facsimile, e-mail or other means of electronic transmission shall be deemed to have the same legal effect as delivery of an original signed copy of this Agreement.

A signed copy of this document must be sent with all new submissions. Only one Agreement is required per submission.

CORRESPONDING AUTHOR

Name: Rosemarie Grantyn

Department: Neuroscience Research Center

Institution: Charité - University Medicine Berlin

Title: Prof. Dr. med.

Signature: *R. Grantyn*
Digital unterschrieben von Rosemarie Grantyn
DN: cn=Rosemarie Grantyn, o=Charite-Universitaetsmedizin Berlin, ou,
email=rosemarie.grantyn@charite.de, c=DE
Datum: 2019.04.10 18:37:19 +02'00'

Date:

Please submit a **signed** and **dated** copy of this license by one of the following three methods:
1. Upload an electronic version on the JoVE submission site
2. Fax the document to +1.866.381.2236
3. Mail the document to JoVE / Attn: JoVE Editorial / 1 Alewife Center #200 / Cambridge, MA 02140